Gene Therapy (2004) 11, 1081–1086

www.nature.com/gt

RESEARCH ARTICLE

Long-term correction of hyperphenylalaninemia by AAV-mediated gene transfer leads to behavioral recovery in phenylketonuria mice

S Mochizuki[1,2], H Mizukami[1], T Ogura[1], S Kure[3], A Ichinohe[3], K Kojima[3], Y Matsubara[3], E Kobayahi[4], T Okada[1], A Hoshika[2], K Ozawa[1,5] and A Kume[1]

[1]*Division of Genetic Therapeutics, Center for Molecular Medicine, Jichi Medical School, Tochigi, Japan;* [2]*Department of Pediatrics, Tokyo Medical University, Tokyo, Japan;* [3]*Department of Medical Genetics, Tohoku University Graduate School of Medicine, Sendai, Japan;* [4]*Division of Organ Replacement, Center for Molecular Medicine, Jichi Medical School, Tochigi, Japan; and* [5]*Division of Hematology, Department of Medicine, Jichi Medical School, Tochigi, Japan*

Classical phenylketonuria (PKU) is a metabolic disorder caused by a deficiency of the hepatic enzyme phenylalanine hydroxylase (PAH). If untreated, accumulation of phenylalanine will damage the developing brain of affected individuals, leading to severe mental retardation. Here, we show that a liver-directed PAH gene transfer brought about long-term correction of hyperphenylalaninemia and behavioral improvement in a mouse model of PKU. A recombinant adeno-associated virus (AAV) vector carrying the murine PAH cDNA was constructed and administered to PAH-deficient mice (strain PAH^{enu2}) via the portal vein. Within 2 weeks of treatment, the hyperphenylalaninemic phenotype improved and completely normalized in the animals treated with higher vector doses. The therapeutic effect persisted for 40 weeks in male mice, while serum phenylalanine concentrations in female animals gradually returned to pretreatment levels. Notably, this long-term correction of hyperphenylalaninemia was associated with a reversal of hypoactivity observed in PAH^{enu2} mice. While locomotory activity over 24 h and exploratory behavior were significantly decreased in untreated PAH^{enu2} mice compared with the age-matched controls, these indices were completely normalized in 12-month-old male PKU mice with lowered serum phenylalanine. These results demonstrate that AAV-mediated liver transduction ameliorated the PKU phenotype, including central nervous system dysfunctions.
Gene Therapy (2004) **11,** 1081–1086. doi:10.1038/sj.gt.3302262; Published online 1 April 2004

Keywords: *phenylketonuria; adeno-associated virus vector; hyperphenylalaninemia; behavioral recovery*

Introduction

Classical phenylketonuria (PKU; McKusick OMIM 261600) is an autosomal recessive disorder resulting from a deficiency of the liver enzyme phenylalanine hydroxylase (PAH; EC 1. 14.16.1).[1] PAH converts phenylalanine (Phe) to tyrosine with the aid of tetrahydrobiopterin (BH_4), and a deficiency of this enzyme causes accumulation of Phe and abnormal metabolites in the body fluids. If untreated, this condition irreversibly damages the central nervous system (CNS) of the patient, resulting in severe mental retardation. Conventional therapy for PKU consists of dietary restriction of Phe, which can prevent neuronal damage if initiated very early in life. However, the strict and complicated diet is often associated with poor compliance, particularly in adolescents and young adults. Premature termination of the diet leads to declined neuropsychological function, and noncompliance in pregnant women with PKU can produce devastating defects in the offspring referred to as 'maternal PKU syndrome'. A permanent cure is therefore awaited to liberate patients from dietary restrictions, and gene therapy is an attractive novel approach to this goal.

However, previous preclinical studies of PKU gene therapy have revealed that a long-term cure of PKU is a formidable task. Generally, recombinant retroviral vectors cannot deliver the normal PAH gene to the liver at sufficient levels to overcome hyperphenylalaninemia.[2,3] Adenoviral-mediated PAH gene transfer achieved a complete reduction of serum Phe in PKU animals, but the therapeutic effects did not persist and the vector was not effectively readministered due to immune responses against the virus.[4,5] On the other hand, adeno-associated virus (AAV) vectors comprise another class of gene delivery vehicles, which have been shown to stably transduce nondividing cells such as hepatocytes, muscle fibers and neurons.[6–8]

In this study, we evaluated a recombinant AAV vector carrying the PAH gene in a mouse model of PKU (PAH^{enu2} strain).[9–11] A missense mutation (F263S) in the PAH gene was introduced into BTBR mouse strain by chemical mutagenesis, resulting in a loss of enzyme activity. Consequently, the homozygous PAH^{enu2} mice

Correspondence: Dr A Kume, Division of Genetic Therapeutics, Center for Molecular Medicine, Jichi Medical School, 3311-1 Yakushiji, Minamikawachi, Tochigi 329-0498, Japan
Received 24 December 2003; accepted 11 February 2004; published online 1 April 2004

share many phenotypic characteristics with human PKU patients, such as profound hyperphenylalaninemia (>20 mg/dl; normal 1–2 mg/dl), behavioral disturbances and hypopigmentation. Previous work suggested that at least 10% of normal PAH activity would be required to prevent hyperphenylalaninemia in PKU mice.[4,5]

Results

Construction of the recombinant AAV vector

We first evaluated vectors derived from AAV serotypes 1 through 5. Recombinant AAV vectors containing the mouse erythropoietin (Epo) gene were infused into the mouse portal vein, and the serum Epo levels were determined. Among them, the AAV5-derived virion yielded the highest Epo concentration (unpublished results).[12,13] Next, we tested several promoters to drive the Epo gene in the context of AAV5. We found that the CAG promoter was the strongest in transgene expression in the liver (unpublished results).[14] This promoter consists of the human cytomegalovirus (CMV) immediate-early enhancer, the chicken β-actin promoter, and a chicken β-actin/rabbit β-globin composite intron.

Based on these results, we constructed an AAV vector as shown in Figure 1 (AAV5/CAG-mPAH). A recombinant AAV plasmid pAAV5/CAG-mPAH was comprised of the CAG promoter, the murine PAH cDNA and the SV40 late polyadenylation signal flanked by the AAV5 inverted terminal repeats (ITRs shown as hairpin loops in Figure 1). The vector DNA was then packaged into the AAV5 capsid through an adenovirus-free, transient transfection protocol.[15]

Correction of hyperphenylalaninemia

For liver-targeted gene transfer, the vector was injected into 5–7-week-old PAH^{enu2} mice via the portal vein. We injected male PKU mice with 3×10^{12} vector genomes (vg) ($n=3$), 1×10^{13} vg ($n=4$), 3×10^{13} vg ($n=3$) or 1×10^{14} vg ($n=3$) of AAV5/CAG-mPAH per animal. Female PKU mice were infused with 1×10^{13} vg ($n=4$), 3×10^{13} vg ($n=4$) or 1×10^{14} vg ($n=5$) per animal.

Serum Phe levels were determined prior to the infusion, biweekly until 12 weeks postinfusion, and every 4 weeks thereafter (Figure 2). Before gene transfer (week 0), all PAH-deficient mice showed profound hyperphenylalaninemia (33.7±3.4 mg/dl; range 29.3–43.5 mg/dl; $n=27$). The degree of hyperphenylalaninemia was not significantly different between males (33.2±2.6 mg/dl; $n=14$) and females (34.3±4.1 mg/dl; $n=13$). Figure 2a shows the kinetics of blood Phe in male PKU mice receiving different doses of AAV5/CAG-mPAH. A striking decrease in serum Phe was observed 2-4 weeks after gene transfer. With the lowest vector dose (3×10^{12} vg), serum Phe was only slightly lowered after 2 weeks (from 35.0±1.6 to 28.1±7.0 mg/dl; $P=0.18$ by paired t-test), but was significantly lowered after 4 weeks (15.6±6.9 mg/dl; $P=0.027$ by paired t-test). With higher vector doses (1×10^{13}, 3×10^{13} and 1×10^{14} vg), the serum Phe level was clearly lowered ($P=0.001$, 0.006 and 0.002 by paired t-test, respectively) to a therapeutic range (<10 mg/dl) in 2 weeks. At 4 weeks postinfusion, each cohort of male mice recorded the lowest serum Phe. In particular, it was completely normalized in the mice treated with 3×10^{13} vg (1.4±0.5 mg/dl) and 1×10^{14} vg (1.2±0.5 mg/dl) of AAV5/CAG-mPAH.

The reduced serum Phe levels were stably maintained for 40 weeks. Complete correction of hyperphenylalaninemia (<2 mg/dl) persisted in the mice treated with the highest vector dose (1×10^{14} vg), and the mice receiving

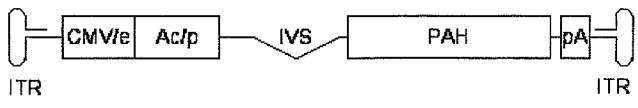

Figure 1 Structure of the AAV5/CAG-mPAH vector. The vector consisted of a CMV immediate-early enhancer (CMV/e), the chicken β-actin promoter (Ac/p), a chicken β-actin/rabbit β-globin composite intron (IVS), the 1.4 kb murine PAH cDNA (PAH) and the SV40 late polyadenylation signal (pA) flanked by the AAV5 inverted terminal repeats (ITRs shown as hairpin loops).

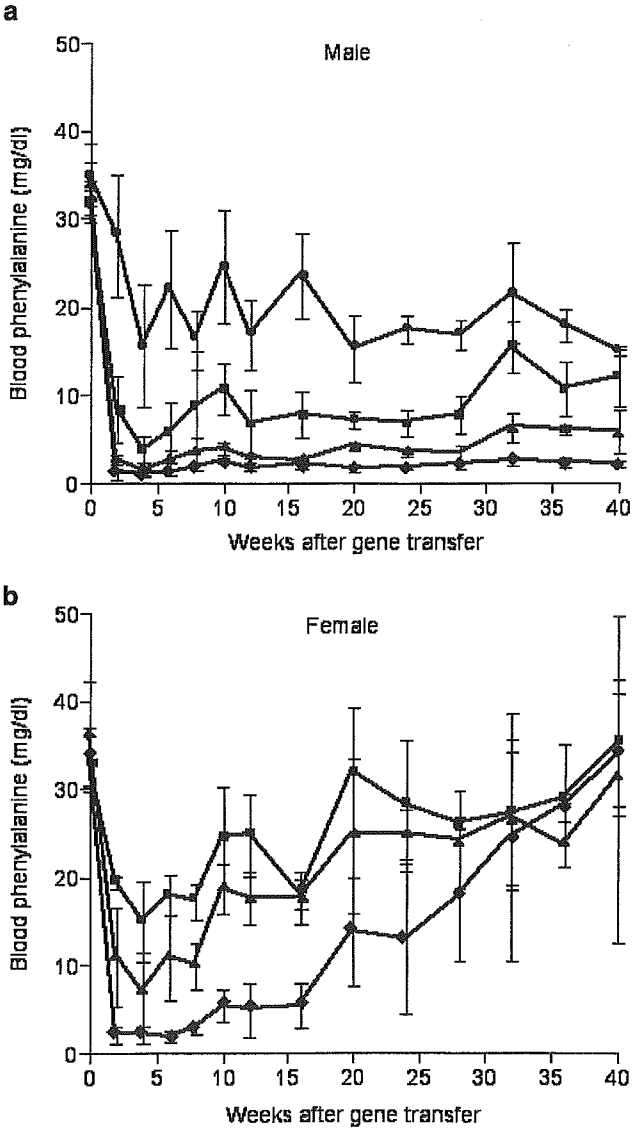

Figure 2 Persistence of the recombinant AAV-mediated correction of hyperphenylalaninemia in male (a) and female (b) PKU mice. Serum Phe concentration was determined prior to vector infusion (week 0) and periodically after gene transfer, and represented as the mean±s.d. for each treatment group. The applied vector dose was 3×10^{12} vg (circles), 1×10^{13} vg (squares), 3×10^{13} vg (triangles) or 1×10^{14} vg (diamonds) per animal.

the second highest dose (3×10^{13} vg) stayed in a well-controlled therapeutic range (<6 mg/dl). Mice receiving lower vector doses (3×10^{12} and 1×10^{13} vg) showed moderate correction of hyperphenylalaninemia, with significant long-term efficacy of the single AAV infusion.

Figure 2b shows the kinetics of serum Phe in female PKU mice after receiving 1×10^{13}, 3×10^{13} or 1×10^{14} vg of AAV5/CAG-mPAH. The vector administration was effective in the female PKU mice, too, but the dose–response and duration were different from the male mice; that is, about three times more vector was required for the female mice to exhibit an equivalent reduction in serum Phe (Figure 3). At 4 weeks postinfusion when the reduction was at its maximum, 1×10^{13} vg of AAV5/CAG-mPAH lowered serum Phe by 50% in the female mice, while the same level of reduction was achieved by 3×10^{12} vg in the males. Similarly, an 80% reduction was achieved by 3×10^{13} vg in the females, whereas only 1×10^{13} vg were required in the males. Complete correction of hyperphenylalaninemia was achieved by 1×10^{14} vg in the females, while it was achieved by 3×10^{13} vg as well as 1×10^{14} vg in the males. As for duration, the therapeutic effect did not persist in the female PKU mice as seen in the males. Serum Phe levels in each female cohort remained low until 8 weeks post-gene transfer, but gradually rose thereafter. With vector doses of 1×10^{13} and 3×10^{13} vg, serum Phe was greater than 20 mg/dl at 20 weeks, and returned to the pretreatment level at 40 weeks. With the highest dose (1×10^{14} vg), serum Phe was kept below 10 mg/dl until 16 weeks, then gradually increased and returned to the pretreatment level at 40 weeks.

Although we did not kill the animals for enzyme assay, previous studies on adenoviral-mediated gene transfer to PAH^{enu2} mice allowed us to estimate the PAH activity accomplished by our vector. These studies showed, in good agreement, that the threshold PAH activity to correct hyperphenylalaninemia was about 10% of normal mice.[4,5] As shown in Figure 3, male PKU mice given 3×10^{12} vg and females given 1×10^{13} vg of the vector showed 50–60% reduction in serum Phe; we speculate that these mice would express about 5% of normal PAH activity. On the other hand, male PKU mice given 3×10^{13} or 1×10^{14} vg and females given 1×10^{14} vg completely recovered from hyperphenylalaninemia, hence their liver PAH activities would be 10% of normal or greater. Male PKU mice given 1×10^{13} vg (ca. 90% reduction in serum Phe) and females given 3×10^{13} vg of AAV (ca. 80% reduction) would have 5–10% of normal PAH activity.

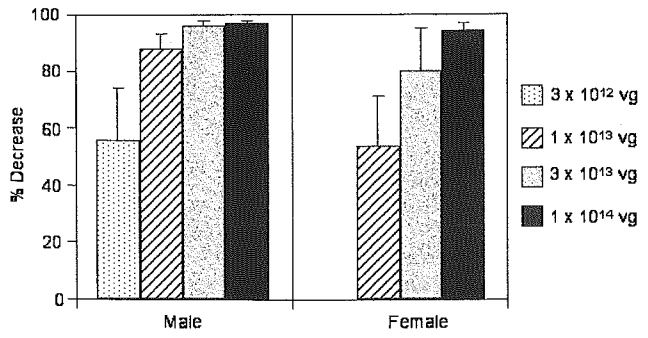

Figure 3 Vector dose-dependent reduction of serum Phe in PKU mice. Percent reduction of serum Phe was calculated by the following formula: {(serum Phe at week 0)−(serum Phe at 4 weeks)} × 100/(serum Phe at week 0). Bars represent the mean ± s.d. of % reduction of serum Phe in PKU mice treated with 1×10^{12} vg (dotted bar), 1×10^{13} vg (hatched bar), 3×10^{13} vg (gray bar), or 1×10^{14} vg of AAV5/CAG-mPAH (black bar).

Correction of hypopigmentation

Associated with extended reductions in serum Phe, hypopigmentation in the AAV-treated PKU mice was ameliorated. While the coat color of untreated mice remained grayish brown, hair darkening in the mice receiving higher vector doses was observed 2 weeks post-transduction, and the mice grew black hair in 4 weeks which was indistinguishable from that of wild-type (WT) BTBR mice (Figure 4). Male PKU mice with reduced serum Phe retained black hair throughout the observation period, while female PKU mice lost pigmentation as the therapeutic effect diminished.

Recovery from hypoactivity following PAH gene transfer

Along with persistent correction of hyperphenylalaninemia and hypopigmentation, we observed behavioral

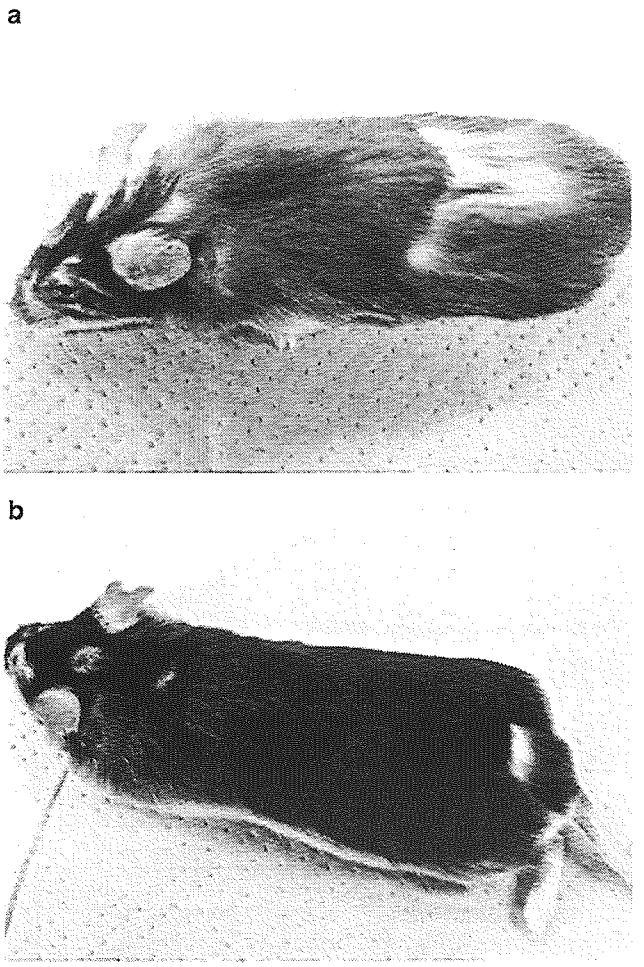

Figure 4 Correction of hypopigmentation in PKU mouse following PAH gene transfer. (a) Untreated PKU mouse showing grayish brown hair, easily distinguished from wild-type and PAH$^{+/-}$ heterozygous BTBR mice. (b) By 8 weeks after PAH gene transfer, the PKU mouse with complete correction of hyperphenylalaninemia recovered black coat color and was indistinguishable from normal BTBR mice.

recovery in AAV-treated PKU mice. Consistent with previous studies showing abnormal behavior and cognitive deficits in PAH^{enu2} mice,[9,16,17] we found that untreated PKU (PAH$^{-/-}$) mice were relatively hypoactive compared with WT (PAH$^{+/+}$) and heterozygous carrier (PAH$^{+/-}$) animals. The hypoactivity became apparent with aging, and the difference was significant among animals aged 10 months or older. Figure 5 shows the results of behavior tests on the 12-month-old animals. As for total locomotion over 24 h, the untreated PKU mice displayed about 70% of normal activity (Figure 5a, $P<0.01$ by Student's *t*-test). On the other hand, the AAV-administered male mice without hyperphenylalaninemia exhibited significantly higher 24-h locomotion than the untreated mice (Figure 5a, $P=0.001$ by Student's *t*-test). Indeed, the AAV-treated animals showed a normal activity level in this test.

Similarly, PAH gene transfer improved the PKU animals' exploratory activity in a novel environment.

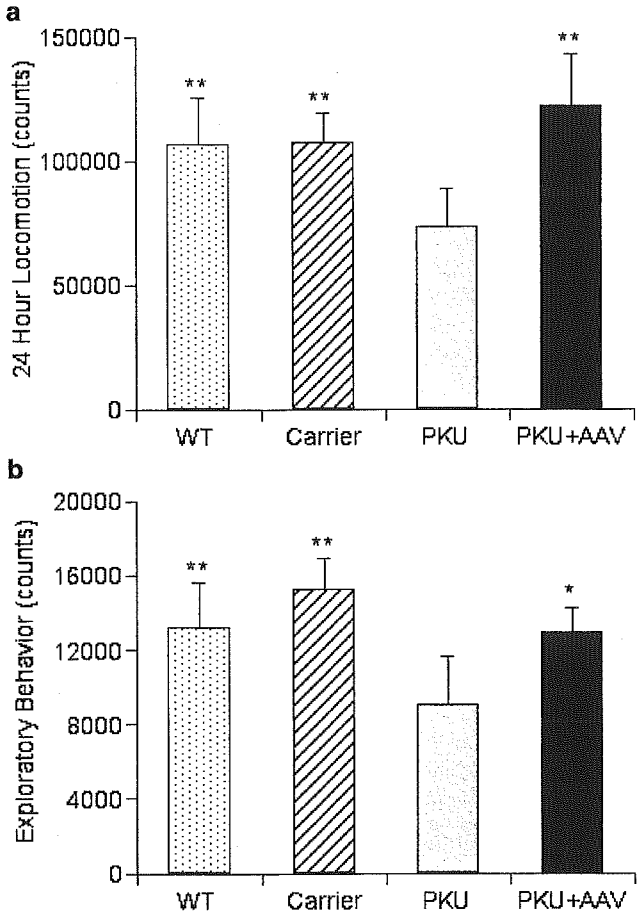

*Figure 5 Recovery from hypoactivity following PAH gene transfer. (a) Total locomotion over 24 h. Mice were placed under an infrared sensor and ambulatory activity was recorded consecutively for 24 h. Wild-type (WT), heterozygous and AAV-treated PKU mice exhibited significantly higher locomotory activity than untreated PKU mice (**$P<0.01$ by Student's t-test). (b) Exploratory behavior. Mice were placed in a novel cage under a sensor and ambulatory activity was quantified during the first 2 h in the chamber. This test showed significantly higher performance by WT, heterozygous and AAV-treated PKU mice than untreated PKU animals (**$P<0.01$ and *$P<0.05$ by Student's t-test). Bars represent the mean±s.d. of WT mice (WT; dotted bar), heterozygous mice (Carrier; hatched bar), untreated PKU mice (PKU; gray bar), and AAV-transduced PKU mice (PKU+AAV; black bar).*

When settled in a novel cage, the untreated PKU males showed 60–70% of normal exploratory activity (Figure 5b, $P<0.01$). On the other hand, PKU mice that had recovered from hyperphenylalaninemia explored as vigorously as WT animals, and their activity level was significantly greater than that of untreated PKU mice ($P=0.015$). These results clearly indicate that the PAH gene transfer improved the CNS function of PKU mice in addition to correction of hyperphenylalaninemia.

Discussion

In this study, we demonstrated that AAV-mediated transduction of the PKU mouse liver brought about a long-term cure of the disease. A single infusion of AAV5/CAG-mPAH completely normalized the hyperphenylalaninemic phenotype in male PKU mice, and the longevity of the therapeutic effect was superior to any other gene delivery vehicle thus far. Although not thoroughly investigated, the result suggests that the transgene was transcriptionally active during observation, and that no significant immune response was elicited against the transduced hepatocytes in the animals. In addition, infusion of very large amounts of AAV did not show any toxicity in the treated mice. The vector safety and viability may be further improved by adopting recently developed purification methods, such as iodixanol gradient, affinity or ion-exchange chromatography.[18–21]

A major problem we encountered in this study was that the same AAV vector was less effective in female PKU mice. About three times more vector was required to achieve an equivalent reduction of serum Phe seen in males, and the therapeutic effect was shorter in duration. The underlying mechanisms for these female-specific phenomena are currently unknown. Davidoff *et al*[22] recently reported similar observations that AAV2- and AAV5-derived vectors less efficiently transduced livers of female mice than males. They suggested that the difference was due to an androgen-dependent pathway for augmenting hepatocyte transduction, but its mode of action is undetermined. Since precise molecular events involved in recombinant AAV-mediated transduction remain obscure, the critical step accounting for the observed sex difference is also a mystery. Androgen may augment the uptake of AAV particles into the cell or traffic them to the nucleus; alternatively, it may stabilize the AAV genome in an episomal state, or enhance vector integration into the host chromosome. Of these possibilities, the last one is less likely, because only a small fraction (<10%) of recombinant AAV genome was reportedly integrated into the mouse hepatocytes.[23] If there is an androgen-dependent mechanism to retain the AAV genome in an episomal state in the liver, lack of such machinery would allow gradual loss of the vector DNA in females, thereby transgene-derived PAH activity would descend over time as we observed. Other possibilities accounting for the lower therapeutic efficacy include transcriptional silencing and an immune response against AAV-transduced hepatocytes, although the latter is unlikely to occur only in female mice.

In genetic treatment of autosomal and acquired disorders, sex-dependent transduction raises a novel issue. Development of more efficient vectors may over-

come this problem, or other approaches can be considered. In terms of PKU, the disease-associated pathology is caused by accumulated Phe in the body fluids. Thus, it can be prevented by 'heterologous gene therapy', ie targeting tissues other than hepatocytes. Several investigators have exploited this strategy because of difficulties with liver transduction and safety concerns. Christensen *et al*[24] transduced primary keratinocytes with genes for PAH and GTP cyclohydrolase I, which is the rate-limiting enzyme in BH_4 biosynthesis. They showed that the cells cleared excess Phe in the culture medium, and suggested that engraftment of enough of these cells may function as a metabolic sink for detoxification. Harding *et al*[25] investigated the potential of skeletal muscle as a PAH-expressing organ. Using a transgenic technique, they created mice expressing PAH in the skeletal muscle but not in the liver. These mice showed hyperphenylalaninemia at baseline, but serum Phe significantly decreased when the animals were supplemented with BH_4. A similar approach to bone marrow cells was unsuccessful,[26] and careful consideration is required in translating these transgenic studies into human applications.

A novel finding in this study was that AAV infusion lead to behavioral improvement in addition to correction of hyperphenylalaninemia and hypopigmentation. To our knowledge, this is the first demonstration that a gene-based approach to PKU actually benefited CNS function. It has been reported that free amino acid and amine contents are dramatically reduced in the PAH^{enu2} mouse brain, as in untreated human PKU patients.[27,28] Presumably, the observed hypoactivity in older PKU mice was associated with the abnormal synthesis of biogenic amines, whereas the abnormality was reversed in AAV-treated PKU animals with normal serum Phe. We speculate that the behavioral recovery in these mice represents an analogous situation in which dietary restriction of Phe can improve some neuropsychiatric symptoms in untreated PKU patients. It is of particular interest whether an earlier genetic intervention can prevent irreversible neuronal defects in PKU and preserve more sophisticated CNS function such as memory. The AAV vectors and PAH^{enu2} mice will provide an attractive system to address such prompting questions.

Materials and methods

AAV vector construction

To isolate murine PAH cDNA (GenBank Accession # NM008777), liver mRNA was prepared from a C57BL/6J mouse (from Clea Japan, Tokyo, Japan) with Isogen reagent (Nippon Gene, Toyama, Japan) and an mRNA Purification kit (Amersham Pharmacia Biotech, Little Chalfont, UK). The PAH cDNA was cloned by reverse transcriptase-directed polymerase chain reaction using a Superscript II cDNA synthesis kit (Invitrogen, Grand Island, NY, USA). The CAG promoter was derived from pCAGGS (a gift from Dr J Miyazaki, Osaka University, Osaka, Japan).[14] The AAV5 vector plasmid pAAV5LacZ and a helper plasmid 5RepCapA were generous gifts from Dr JA Chiorini (National Institutes of Health, Bethesda, MD, USA).[12] To construct a recombinant AAV5 vector plasmid for PAH expression, the expression cassette of pAAV5LacZ was replaced with the CAG promoter, the murine PAH cDNA and the SV40 late polyadenylation signal, and the plasmid was referred to as pAAV5/CAG-mPAH (Figure 1).

Recombinant AAV stocks were propagated according to an adenovirus-free, three-plasmid transfection protocol described previously.[15] Briefly, subconfluent 293 cells (4×10^8 cells per 10 trays) in Cell Factories 10 (Nunc, Roskilde, Denmark) were cotransfected with 650 μg of the vector plasmid pAAV5/CAG-mPAH, 650 μg of the AAV helper plasmid 5RepCapA and 650 μg of the adenoviral helper plasmid pLadeno1 (identical to pVAE2AE4-2 in Matsushita *et al*;[15] kindly provided by Avigen, Alameda, CA, USA) by using the calcium phosphate precipitation method for a period of 6 h. Cells were harvested 72 h after transfection and lysed by three freeze–thaw cycles. The crude viral lysate was incubated with Benzonase (Merck KGaA, Darmstadt, Germany) and centrifuged. Finally, the clear supernatant was subjected to two rounds of CsCl density-gradient ultracentrifugation for purification. The physical titer of the viral stock was determined by DNA dot blot and hybridization with the murine PAH cDNA probe, along with plasmid standards. Typically, we obtained 5×10^{13} vg of AAV5/CAG-mPAH from a culture container (10 trays).

Transduction of mouse liver

All animal experiments were carried out in accordance with our institutional guidelines. PAH^{enu2} mice were generous gifts from Dr T Shiga (University of Tsukuba, Tsukuba, Japan), and a colony was established at Jichi Medical School (Tochigi, Japan). PKU mice used for *in vivo* gene transfer were 5–7 weeks of age. Mice were anesthetized with isoflurane inhalation followed by laparotomy. A 300 μl of saline suspension containing 3×10^{12}–1×10^{14} vg of AAV5/CAG-mPAH was slowly injected into the portal vein using an insulin syringe with a 29-gauge needle (Terumo, Tokyo, Japan).

Serum Phe assay

Serum Phe was measured by an enzymatic microfluorometric assay using an Enzaplate PKU-R kit (Bayer Medical, Tokyo, Japan). Mice were tail phlebotomized and the blood was spotted onto a mass-screening grade paper filter (#545, provided by Advantec Toyo, Tokyo, Japan). A 3 mm diameter disc was punched out from the dried blood spot and placed in a 96-well plate. Phe was eluted from the disc and incubated with Phe dehydrogenase, an NAD-dependent enzyme, and resazurin. The enzyme reaction produces NADH, which in turn converts resazurin to resorufin with the aid of diaphorase. The resultant resorufin was measured on a Fluoroskan Ascent plate reader (Labsystems, Helsinki, Finland) with a 544/590 nm filter set.

Mouse behavior tests

Mice were tested at 12 months of age. To measure locomotory activity over 24 h, the home cage of the mouse was placed under an infrared sensor that detects thermal radiation from animals (Supermex; Muromachi Kikai, Tokyo, Japan).[29] Ambulation was scored by a personal computer interfaced to the sensor. Alternatively, exploratory behavior was tested by placing the mouse in a novel cage under the infrared sensor.

Ambulatory activity was quantified during the first 2 h in the chamber.

Acknowledgements

We are grateful to Dr JA Chiorini for pAAV5LacZ and 5RepCapA, Dr J Miyazaki for pCAGGS, Dr T Shiga for PAH^{enu2} mice, Avigen for pLadeno1, and Advantec Toyo for #545 filter paper. We also thank Dr Y Hakamata for technical assistance in the animal experiments. This work was supported in part by grants from the Ministry of Education, Culture, Sports, Science and Technology, and the Ministry of Health, Labor and Welfare, Japan.

References

1 Scriver CR, Kaufman S. Hyperphenylalaninemia: phenylalanine hydroxylase deficiency. In: Scriver CR, Beaudet AL, Sly WS, Valle D (eds) *The Metabolic and Molecular Basis of Inherited Diseases*. McGraw-Hill: New York, 2001, pp 1667–1724.
2 Liu T-J, Kay MA, Darlington GJ, Woo SLC. Reconstitution of enzymatic activity in hepatocytes of phenylalanine hydroxylase-deficient mice. *Somat Cell Mol Genet* 1992; **18**: 89–96.
3 Eisensmith RC, Woo SLC. Gene therapy for phenylketonuria. *Eur J Pediatr* 1996; **155** (Suppl 1): S16–S19.
4 Fang B *et al*. Gene therapy for phenylketonuria: phenotypic correction in a genetically deficient mouse model by adenovirus-mediated hepatic gene transfer. *Gene Therapy* 1994; **1**: 247–254.
5 Nagasaki Y *et al*. Reversal of hypopigmentation in phenylketonuria mice by adenovirus-mediated gene transfer. *Pediatr Res* 1999; **45**: 465–473.
6 Nathwani AC *et al*. Sustained high-level expression of human factor IX (hFIX) after liver-targeted delivery of recombinant adeno-associated virus encoding the hFIX gene in rhesus macaques. *Blood* 2002; **100**: 1662–1669.
7 Kay MA *et al*. Evidence for gene transfer and expression of factor IX in haemophilia B patients treated with an AAV vector. *Nat Genet* 2000; **24**: 257–261.
8 Muramatsu S *et al*. Behavioral recovery in a primate model of Parkinson's disease by triple transduction of striatal cells with adeno-associated viral vectors expressing dopamine-synthesizing enzymes. *Hum Gene Ther* 2002; **13**: 345–354.
9 Shedlovsky A, McDonald JD, Symula D, Dove WF. Mouse models of human phenylketonuria. *Genetics* 1993; **134**: 1205–1210.
10 McDonald JD, Charlton CK. Characterization of mutations at the mouse phenylalanine hydroxylase locus. *Genomics* 1997; **39**: 402–405.
11 McDonald JD *et al*. The phenylketonuria mouse model: a meeting review. *Mol Genet Metab* 2002; **76**: 256–261.
12 Chiorini JA, Kim F, Yang L, Kotin RM. Cloning and characterization of adeno-associated virus type 5. *J Virol* 1999; **73**: 1309–1319.
13 Mingozzi F *et al*. Improved hepatic gene transfer by using an adeno-associated virus serotype 5 vector. *J Virol* 2002; **76**: 10497–10502.
14 Niwa H, Yamamura K, Miyazaki J. Efficient selection for high-expression transfectants with a novel eukaryotic vector. *Gene* 1991; **108**: 193–200.
15 Matsushita T *et al*. Adeno-associated virus vectors can be efficiently produced without helper virus. *Gene Therapy* 1998; **5**: 938–945.
16 Zagreda L *et al*. Cognitive deficits in a genetic mouse model of the most common biochemical cause of human mental retardation. *J Neurosci* 1999; **19**: 6175–6182.
17 Cabib S *et al*. The behavioral profile of severe mental retardation in a genetic mouse model of phenylketonuria. *Behav Genet* 2003; **33**: 301–310.
18 Hermens WT *et al*. Purification of recombinant adeno-associated virus by iodixanol gradient ultracentrifugation allows rapid and reproducible preparation of vector stocks for gene transfer in the nervous system. *Hum Gene Ther* 1999; **10**: 1885–1891.
19 Zolotukhin S *et al*. Recombinant adeno-associated virus purification using novel methods improves infectious titer and yield. *Gene Therapy* 1999; **6**: 973–985.
20 Auricchio A, O'Connor E, Hildinger M, Wilson JM. A single-step affinity column for purification of serotype-5 based adeno-associated viral vectors. *Mol Ther* 2001; **4**: 372–374.
21 Kaludov N, Handelman B, Chiorini JA. Scalable purification of adeno-associated virus type 2, 4, or 5 using ion-exchange chromatography. *Hum Gene Ther* 2002; **13**: 1235–1243.
22 Davidoff AM *et al*. Sex significantly influences transduction of murine liver by recombinant adeno-associated viral vectors through an androgen-dependent pathway. *Blood* 2003; **102**: 480–488.
23 Nakai H *et al*. Extrachromosomal recombinant adeno-associated virus vector genomes are primarily responsible for stable liver transduction *in vivo*. *J Virol* 2001; **75**: 6969–6976.
24 Christensen R, Kolvraa S, Blaese RM, Jensen TG. Development of a skin-based metabolic sink for phenylalanine by overexpression of phenylalanine hydroxylase and GTP cyclohydrolase in primary human keratinocytes. *Gene Therapy* 2000; **7**: 1971–1978.
25 Harding CO *et al*. Metabolic engineering as therapy for inborn errors of metabolism – development of mice with phenylalanine hydroxylase in muscle. *Gene Therapy* 1998; **5**: 677–683.
26 Harding CO *et al*. Expression of phenylalanine hydroxylase (PAH) in erythrogenic bone marrow does not correct hyperphenylalaninemia in *Pah^{enu2}* mice. *J Gene Med* 2003; **5**: 984–993.
27 Puglisi-Allegra S *et al*. Dramatic brain aminergic deficit in a genetic mouse model of phenylketonuria. *NeuroReport* 2000; **11**: 1361–1364.
28 Pascucci T, Ventura R, Puglisi-Allegra S, Cabib S. Deficits in brain serotonin synthesis in a genetic mouse model of phenylketonuria. *NeuroReport* 2002; **13**: 2561–2564.
29 Masuo Y, Matsumoto Y, Morita S, Noguchi J. A novel method for counting spontaneous motor activity in the rat. *Brain Res Protoc* 1997; **1**: 321–326.

Liver Tissue Engineering at Extrahepatic Sites in Mice as a Potential New Therapy for Genetic Liver Diseases

Kazuo Ohashi,[1,3] Jacob M. Waugh,[2] Michael D. Dake,[2] Takashi Yokoyama,[3] Hiroyuki Kuge,[3] Yoshiyuki Nakajima,[3] Masaki Yamanouchi,[4] Hiroyuki Naka,[4] Akira Yoshioka,[4] and Mark A. Kay[1]

Liver tissue engineering using hepatocyte transplantation has been proposed as an alternative to whole-organ transplantation or liver-directed gene therapy to correct various types of hepatic insufficiency. Hepatocytes are not sustained when transplanted under the kidney capsule of syngeneic mice. However, when we transplanted hepatocytes with the extracellular matrix components extracted from Engelbreth-Holm-Swarm cells, hepatocytes survived for at least 140 days and formed small liver tissues. Liver engineering in hemophilia A mice reconstituted 5% to 10% of normal clotting activity, enough to reduce the bleeding time and have a therapeutic benefit. Conversely, the subcutaneous space did not support the persistent survival of hepatocytes with Engelbreth-Holm-Swarm gel matrix. We hypothesized that establishing a local vascular network at the transplantation site would reduce graft loss. To test this idea, we provided a potent angiogenic agent before hepatocyte transplantation into the subcutaneous space. With this procedure, persistent survival was achieved for the length of the experiment (120 days). To establish that these engineered liver tissues also retained their native regeneration potential *in vivo*, we induced two different modes of proliferative stimulus to the naïve liver and confirmed that hepatocytes within the extrahepatic tissues regenerated with activity similar to that of naïve liver. In conclusion, our studies indicate that liver tissues can be engineered and maintained at extrahepatic sites, retain their capacity for regeneration *in vivo*, and used to successfully treat genetic disorders. (HEPATOLOGY 2005; 41:132–140.)

Development of cellular-based therapies, including hepatocyte transplantation and liver tissue engineering, has been attempted to treat different forms of liver diseases as an alternative to liver organ transplantation.[1–4] By transplanting isolated hepatocytes through the portal circulation into the liver, encouraging results were reported in patients with Criglar-Najjar syndrome and a glycogen storage disease.[1,2] However, this approach of cell transplantation through the portal vein is limited in the number of cells that can be transplanted at one time because of potential life-threatening complications.[3,5,6] To increase the utility of hepatocyte-based therapy, it is important to develop a method that allows for the engraftment of a greater number of hepatocytes. In this context, transplanting hepatocytes at an extrahepatic site is attractive because it would provide additional space to maintain a greater number of cells, and with fewer complications.[3,7–9] This type of approach is extremely viable from the standpoint of liver tissue engineering. Researchers have transplanted hepatocytes at several different extrahepatic sites, including the intraperitoneal cavity, pancreas, mesenteric leaves, lung parenchyma, under the kidney capsule, and in the subcutaneous space.[3,5,8,10,11] Irrespective of the sites used, the studies reported inefficient engraftment of hepatocytes and very short-term survival. To overcome this issue, we have recently used an agonistic antibody that stimulates the HGF/cMet pathway to achieve persistent survival of human hepatocytes (>140 days) grafted into mice under the kidney capsule space.[8,12] These successes have encouraged us to establish more clinically feasible methods for liver tissue engineering at

Abbreviations: hAAT, human alpha-1 antitrypsin; EHS, Engelbreth-Holm-Swarm; aFGF, acidic fibroblast growth factor; MS, microspheres; DH, direct hyperplasia; TCPOBOP, 1,4-bis[2-(3,5-dicholoropyridyloxy)] benzene; BrdU, 5-bromo-2-deoxyuridine.

From the Departments of [1]Pediatrics and Genetics and [2]Cardiovascular and Interventional Radiology, Department of Radiology, Stanford University Medical Center, Stanford, CA; and the [3]First Department of Surgery and [4]Department of Pediatrics, Nara Medical University, Nara, Japan.

Received April 26, 2004; accepted September 20, 2004.

Supported by NIH U19-AI40034 (M.A.K.), Grant-in-Aid from the Scientific Research from the Ministry of Education, Science, Sports and Culture of Japan (Y.N. and K.O.), and Japan Society for the Promotion of Science Fellowship (K.O.).

Address reprint requests to: Mark A. Kay, M.D., Ph.D., Departments of Pediatrics and Genetics, Stanford University Medical Center, Rm G305, 300 Pasteur Dr., Stanford, CA 94305-5208. E-mail: markay@stanford.edu; fax: 650-498-6540.

Published online in Wiley InterScience (www.interscience.wiley.com).

DOI 10.1002/hep.20484

Conflict of interest. Nothing to report.

extrahepatic sites that do not require the administration of additional compounds.

Materials and Methods

Hepatocyte Isolation. Hepatocytes were isolated from 10- to 15-week-old human alpha-1 antitrypsin (hAAT) transgenic mice (hA1AT-FVB/N, kindly provided by Dr. Bumgardner, Ohio State University, Columbus, OH) by *in situ* collagenase perfusion (Collagenase D, Boehringer Mannheim, Indianapolis, IN) of the liver through the inferior vena cava.[3,8] Cells were filtered and hepatocytes were separated from nonparenchymal cells by 3 rounds of low-speed centrifugation at 50*g*. Hepatocytes with viabilities more than 80%, as quantified by trypan blue exclusion, were used in the present studies. Cells were stored at 4°C before transplantation. Hepatocytes also were isolated from C57Bl/6 mice (CLEA Japan Inc., Tokyo, Japan) for the hemophilia mouse study.

Transplantation Procedures. All animal studies used the institutional guidelines set forth by Stanford University and the Nara Medical University Animal Care Committee. In all studies except for the hemophilia A mouse experiments, FVB/N mice (Jackson Laboratories, Bar Harbor, ME) were used as a recipient. Right before the cell transplantation, hA1AT-FVB/N hepatocytes were resuspended (to a ratio of 1×10^7 cells per milliliter) with cold Williams E Medium (Invitrogen Corp., Carlsbad, CA) without serum or with an equal volume of Williams E Medium and cold Engelbreth-Holm-Swarm (EHS) gel (Matrigel, BD Biosciences, Bedford, MA). For under-the-kidney capsule transplantation, a total of 3×10^6 hepatocytes were transplanted by dividing the dose between the two kidney capsule spaces. For subcutaneous transplantation, 6×10^6 hepatocytes were transplanted into the subcutaneous space between the scapulae. Because EHS-gel quickly polymerizes into a 3-dimensional gel at room temperature, all of the procedures were done at 4°C. In some experiments, we placed acidic fibroblast growth factor microspheres (aFGF-MS) (described below) into the subcutaneous space of the back and transplanted hepatocytes at the same location 10 days afterwards.

In the hemophilia mouse study, we used a mouse model of hemophilia A in the C57Bl/6 background, that lack functional factor VIII activity (kindly provided by Dr. Kazazian Jr., University of Pennsylvania, Philadelphia, PA). Hepatocytes were isolated from C57Bl/6 mice as a syngeneic combination. Hepatocytes resuspended with EHS-gel then were transplanted into either the unilateral or the bilateral kidney capsule spaces of factor VIII–deficient hemophilia mice at a ratio of 1.5×10^6 per kidney.[13] To avoid uncontrolled bleeding during surgery, we infused 90 U/kg factor VIII concentrates into the peritoneum (Confact F, Chemo-Sero-Therapeutic Inc., Kumamoto, Japan), 30 minutes before the hepatocyte transplantation or sham operation. The half-life of the infused factor VIII was less than 12 hours.

Measurement of the Mice Factor VIII Activity. The serum factor VIII biological activity was quantitated by the 1-step clotting assay based on the activated partial thrombin time using human FVIII-deficient plasma (bioMerieux Inc., Durham, NC). The advantage of this method over the chromogenic assay in terms of accuracy has been previously described.[14] Pooled human plasma (bioMerieux Inc.) was used as the FVIII activity standard. Before performing the assay, we confirmed that the FVIII activity in the FVIII-KO mouse pooled plasma represented less than 2%, whereas the activity in the normal pooled mice plasma showed higher than 100% of normal human FVIII activity. All standards and samples were measured in duplicate. Mouse tail-clip bleeding time assay was performed by cutting 1 cm from the tip of the mouse tail.[15] The mouse was returned to a separate cage, and the bleeding time was measured. If the mouse did not stop bleeding at 30 minutes, we cauterized the wounds to save the mouse.

Production of Acidic FGF-Microspheres. To provide local release of growth factor into the subcutaneous space, different doses of potent angiogenic agent, aFGF (R&D Systems, Minneapolis, MN, lot # CQ089111) with stabilization by heparin, were incorporated into the microspheres (MS). Bioerodible polyethylene glycol-polylactide-co-glycolide (Polysciences, Warrington, PA) MS were prepared as a modification of previously described techniques.[16,17] An 8:1 ratio of polylactide-co-glycolide (PLGA; 75:25; Polysciences, Warrington, PA) to PEG-8000 (polyethylene glycol, MW 8000, Sigma, St. Louis, MO) was employed with the double emulsion technique to generate MS of final mean diameter 8 to 10 μm. Additionally, a pH buffer of 7.4 was incorporated in all MS preparations as a modification of other techniques to limit local pH changes. MS were prepared to give a continuous mean daily release of 0 ng (saline), 0.0167 ng, 0.167 ng, and 1.67 ng for 14 days in aFGF-MS-G1, aFGF-MS-G2, aFGF-MS-G3, and aFGF-MS-G4, respectively. All of the groups of MS also incorporated 32 units heparin per 5 mg MS. Five micrograms of MS were resuspended with 250 μL Williams E Medium for 8 hours and injected into the subcutaneous space of the back with admixing 250 μL EHS-gel. Ten days later, we removed the subcutaneous tissues for histological analysis of the vascular network or transplanted hepatocytes at the same location.

Enzyme-Linked Immunosorbent Assay. Recipient serum hAAT concentrations were assayed by using antibody against hAAT (Dia Sorin, Stillwater, MN) as described elsewhere.[8,18]

Liver Proliferation Stimulus. Two different modes of liver proliferation were induced at 70 days after hepatocyte transplantation: (1) Hepatectomy group: compensatory regeneration was induced by performing a two-third partial hepatectomy by surgically removing the median and lateral lobes[19,20] under general anesthesia using methoxyflurane (Metafane, Mallinkrodt, IL); and (2) Direct hyperplasia (DH) group: direct hyperplasia mode of hepatocyte proliferation was induced by a single intragastric injection of the primary mitogen 1,4-bis [2-(3,5-dichloropyridyloxy)] benzene (TCPOBOP, kindly provided by Dr. B. Diwan, National Cancer Institute, Bethesda, MD) at a dose of 3 mg/kg.[19,20] For the analysis of cell cycle proliferation in naïve and engineered livers, we administered 5-bromo-2-deoxyuridine (BrdU) subcutaneously (Sigma, St. Louis, MO) at a dose of 1 mg/d through the use of an osmotic mini-pump (model 2001; Alzet, Palo Alto, CA) for a period of 14 days starting at the same day as giving the regenerative stimulus. Fourteen days later, livers, engineered liver tissues including kidneys and surrounding subcutaneous tissues, and duodenum were removed and processed for histological analysis.

Histological Analysis and Immunohistochemistry. aFGF-MS–treated subcutaneous tissues, livers, engineered liver tissues including kidneys and surrounding subcutaneous tissues, and duodenum (for positive control) were fixed in 10% formalin before embedding into paraffin as previously described.[21] Sections (5 μm) were processed for the following immunohistochemical analysis and hematoxylin & eosin staining. In the aFGF-MS study, vascular numbers were counted at the area surrounding the EHS-gel-plug at 10 randomly selected areas (total of 0.1 mm^2) on the sections stained by hematoxylin & eosin. For immunohistochemistry, after deparaffinization, sections were treated with 3% hydrogen peroxide solution for 20 minutes and then were incubated with 2N HCl for 90 minutes. Nonspecific binding sites were blocked with unconjugated human anti-mouse IgG (Vector Laboratories, Burlingame, CA) and 10% normal goat serum (Vector Laboratories). Sections were incubated overnight at 4°C with mouse anti-BrdU antibody (1:30, Becton Dickinson, San Jose, CA) and rabbit anti-hAAT antibody (1:200, Boehringer Mannheim). After rinses, sections were then incubated for 30 minutes at room temperature with Texas-Red–conjugated goat anti-mouse IgG (1:200, Molecular Probes Inc., Eugene, OR) and FITC-conjugated goat anti-rabbit IgG (1:500, Molecular Probes Inc.). Preparations were counterstained with 4′,6′-diamidino-2-phenylindole (DAPI, 1 μg/mL, Sigma) for 30 minutes, extensively rinsed, mounted, and coverslipped. In each mouse, the BrdU labeling indices of hepatocytes in naïve liver and engineered liver were determined separately by counting a total of 1,000 hepatocytes in 20 to 30 randomly selected liver fields and expressed as a percentage of all positive nuclei. The duodenum was used as a positive control tissue for this experiment.

Statistical Analysis. The significance of differences in the value of hAAT serum between groups were tested by Student *t* test, and differences in the vessel number and BrdU index among groups were tested by a 1-way ANOVA with the use of StatView 5.0 software (SAS Institute Inc., Cary, NC). If a probability *P* value of less than .05 was obtained, the Tukey test was used for comparison for each individual group with the appropriate control.

Results

To engineer liver tissues under the kidney capsule of mice, we isolated hepatocytes from transgenic mice (hA1AT-FVB/N) that express the serum marker protein, human alpha-1 antitrypsin (hAAT) driven by the liver-specific alpha-1 antitrypsin promoter, and transplanted them under the kidney capsule. The maintenance of the transplants *in vivo* was determined by periodic serum measurement of the hAAT transgene product.[4,8,22] The transplanted hepatocytes sharply declined to approximately 30% of the day-3 value by 3 weeks and continuously deteriorated afterward (Fig. 1A). Because extrahepatic sites may lack the proper microenvironment necessary for hepatocyte attachment and differentiation, we studied whether transplanting extracellular matrix components and bound growth factors with the hepatocytes would increase their survival. When we transplanted hepatocytes resuspended in extracellular matrix components extracted from EHS cells, hepatocytes persisted for at least 20 weeks (the length of this experiment; Fig. 1A). Histological examination at week 20 confirmed that the hepatocyte-specific hAAT originated from the transplanted hepatocytes. In addition, these cells showed specific characteristics of differentiated hepatocytes, including periodic acid-Schiff (PAS) staining for glycogen synthesis (Fig. 1B-D). We transplanted the same number of hepatocytes (1.5×10^6 hepatocytes) into two different sites and found that the established kidney capsule hepatocyte transplantation technique resulted in higher survival compared with the hepatocyte transplantation into the liver through the portal vein (Fig. 1E).

To set out to evaluate the liver tissue engineering approach in a clinically relevant model of human disease, we transplanted isogenic wild-type hepatocytes into the kid-

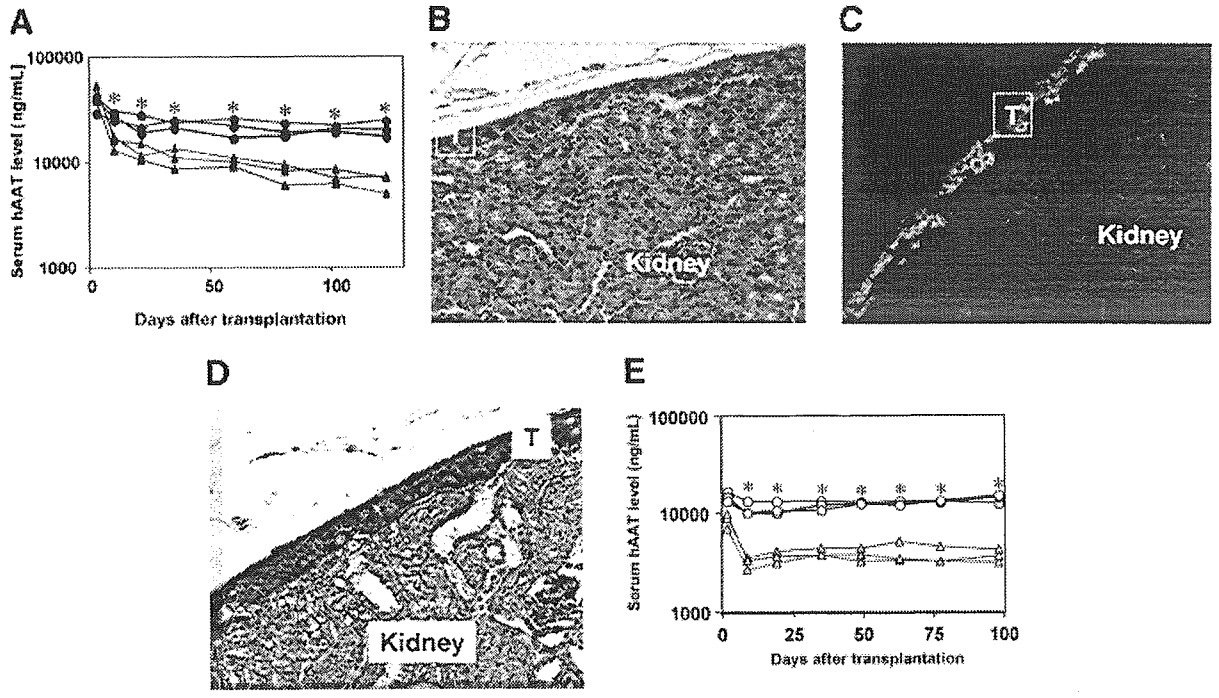

Fig. 1. Engineering extrahepatic liver tissues under the kidney capsule in mice. (A-D) hA1AT-FVB/N mouse hepatocytes were transplanted at day 0. (**closed triangle**, mice received hepatocytes resuspended with WE medium; **closed circle**, mice received hepatocytes resuspended with WE medium plus EHS-gel). (A) Mouse serum hAAT levels after hepatocyte transplantation. $*P < .05$ between WE medium plus EHS-gel group vs. WE medium group at time points of day 9 and thereafter. (B-D) Histological analysis of the transplants at week 20 of mice engrafted hepatocytes resuspended with WE medium plus EHS-gel; hematoxylin-eosin staining (B), hAAT immunostaining (C), or PAS staining (D). Original magnification ×200. T, transplanted hepatocytes. F, Mouse serum hAAT levels after hepatocyte transplantation under the kidney capsule or into the liver through portal vein (**open triangle**, mice received hepatocytes into the liver; **open circle**, mice received hepatocytes resuspended with WE medium plus EHS-gel under the kidney capsule). Each mouse received 1.5×10^6 hepatocytes. $*P < .05$ between groups at time points of day 9 and thereafter.

ney capsule space of factor VIII–deficient hemophilia A mice. Therapeutic levels of factor VIII activity were achieved, reaching approximately 5% and 10% of the normal activity in unilateral and bilateral kidney transplanted groups, respectively (Fig. 2). Hemophilia A mice that underwent a sham operation did not show any detectable serum factor VIII activities after the procedure. In

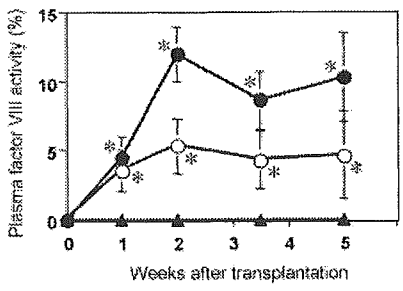

Fig. 2. Plasma factor VIII activities in hemophilia A mice. Isolated C57Bl/6 mouse hepatocytes resuspended with EHS-gel were transplanted under the kidney capsule. Factor VIII-deficient mice received transplants into unilateral (**open circle**), bilateral (**closed circle**) kidney at day 0. Control mice that received a sham operation were used as controls (**closed triangle**).

humans, achievement of these levels of factor VIII would convert a patient from a severe form of the disease to a mild one, basically eliminating the bleeding diathesis except in times of substantial trauma. Nevertheless, to establish phenotypic correction, we measured the bleeding time 2 weeks after the transplantation. The liver-treated mice showed similar bleeding times as the control wild-type mouse group and showed significantly shortened bleeding times compared with the sham-treated mice (13.3 ± 2.1, 18.3 ± 2.9, 16.0 ± 2.9, and 30.0 ± 0.1 minutes, in the wild-type control, unilateral transplant, bilateral transplant, and sham-treated groups of Hemophilia A mice, respectively; $n = 3$ in each group; $P < .01$ sham group versus unilateral or bilateral transplant groups).

Because the liver possesses the ability to undergo active proliferation during pathological states, we studied the potential of the engineered liver tissues for proliferation capacity. We induced two distinct pathways of liver proliferation in the mice 70 days after hepatocellular engraftment into the kidney capsule. Compensatory regeneration was induced by performing a two-third partial

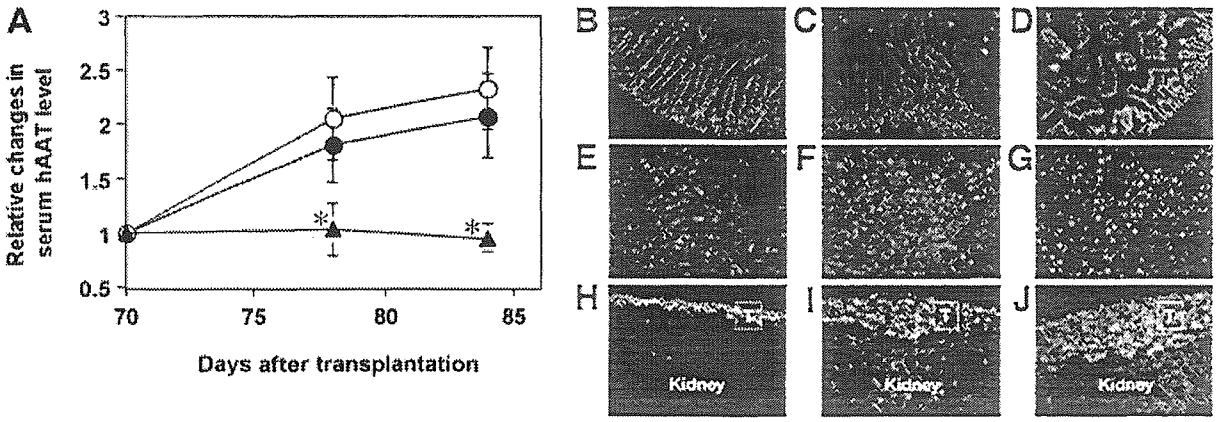

Fig. 3. Proliferation of the naïve liver and liver tissues under the kidney capsule. At day 0, hA1AT-FVB/N mouse hepatocytes resuspended with WE medium plus EHS-gel were transplanted, and at day 70 mice received either two-thirds partial hepatectomy (hepatectomy group) (C, F, I), intragastric injection of TCPOBOP (DH group) (D, G, J), or sham operation as a control (B, E, H). We delivered BrdU continuously for 14 days (days 70-84). (A) Mouse serum hAAT levels after the proliferation stimulus. At days 70, 78, and 84, the serum hAAT levels were measured by enzyme-linked immunosorbent assay, and the relative levels of hAAT were expressed by comparing values with that of at day 70 in each mouse. **Open circle**, mice in the hepatectomy group; **closed circle**, mice in the DH group; **closed triangle**, mice in the control group. $*P < .05$ control group vs. other 2 groups. (B-D) Representative photomicrographs of BrdU immunostaining from duodenum epithelium sections of control group (B), hepatectomy group (C), and DH group (D). BrdU-positive nuclei were colored with Texas red. That all the epithelial cells showed positive staining in their nuclei confirmed that BrdU had continuously been infused. (E-G) Representative photomicrographs of BrdU immunostaining from the naïve liver sections of control group (E), hepatectomy group (F), and DH group (G). (H-J) Representative photomicrographs of BrdU and hAAT co-immunostaining from engrafted hepatocytes in the kidney sections of control group (H), hepatectomy group (I), and DH group (J). hAAT-positive cytoplasm were colored with fluorescein isothiocyanate, and the BrdU-positive nuclei were colored with Texas red. Original magnification, ×100 in B-D and ×200 in E-J.

hepatectomy, and the DH mode of regeneration was induced by intragastric injection of the primary mitogen 1,4-bis [2-(3,5-dichloropyridyloxy)] benzene (TCPOBOP). To assess cell proliferation status of the naive hepatocytes and grafted hepatocytes, BrdU, a cell cycle marker, was administered for 14 days, and BrdU-positive cells were detected by immunohistochemistry. In the naïve liver, the BrdU labeling indexes were 12.1% ± 2.5%, 95.5% ± 3.3%, and 94.9% ± 2.6% in the non–liver manipulated control (control), hepatectomy, and DH groups, respectively (Fig. 3E-G; Table 1). The weight of the naive livers in the hepatectomy group returned to near normal levels, and that of the DH groups showed a significant increase in liver mass compared with the normal liver (data not shown), both of which were consistent with our previous study.[19] In the engineered liver tissues, hepatocytes showed 12.7% ± 2.1%, 91.9% ± 3.3%, and 88.5% ± 3.7% BrdU labeling in the control, hepatectomy, and DH groups, respectively (Fig. 3H-J; Table 1). At day 84 (2 weeks post–proliferative stimulus), we confirmed that the serum hAAT levels in mice increased to 237% ± 18%, and 205% ± 17% in the hepatectomy and DH groups compared with the pretreatment value at day 70 (Fig. 3A).

We next attempted to engineer liver tissues into the subcutaneous space by transplanting hA1AT-FVB/N

Table 1. Regeneration of the Naïve Livers and Extrahepatic Liver Tissues Engineered at the Kidney and Subcutaneous Space (BrdU Was Delivered for 14 Days After Giving Each Mode of Regeneration Stimulus)

Tissue Engineered Site	Mode of Regeneration Stimulus	BrdU LI of Hepatocytes in the Naïve Liver	BrdU LI of Hepatocytes in the Engineered Liver Tissue
Kidney capsule	Control (3)	12.1 ± 2.5	12.7 ± 2.1
	CR (4)	95.5 ± 3.3*	91.9 ± 3.3*
	DH (4)	94.9 ± 2.6*	88.5 ± 3.7*
Subcutaneous space	Control (3)	12.5 ± 3.4	10.5 ± 3.3
	CR (3)	94.2 ± 4.2*	83.3 ± 4.7*
	DH (3)	93.3 ± 4.9*	75.6 ± 6.7*

NOTE. Seventy days after hepatocyte transplantation, we induced liver regeneration. To detect proliferated cells, we delivered BrdU continuously for 14 days through the Osmotic mini-pump. Numbers of mice examined in parentheses.

Abbreviations: CR, compensatory regeneration induced by performing two-third hepatectomy; DH, direct hyperplasia induced by the injection of TCPOBOP.

$*P < .005$ vs. control group.

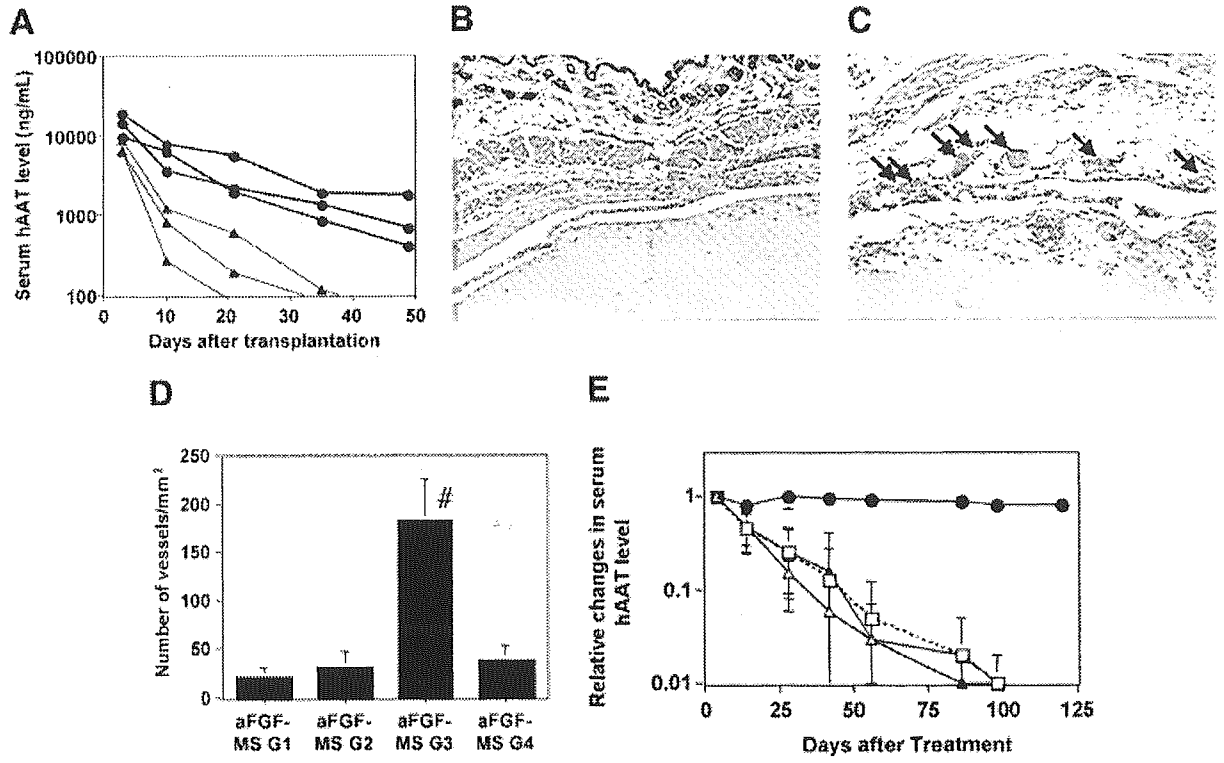

Fig. 4. Engineering extrahepatic liver tissues into the subcutaneous space. (A) Mouse serum hAAT levels after the transplantation. hA1AT-FVB/N mouse hepatocytes were transplanted into the subcutaneous space of the back at day 0 (**closed triangle**, mouse received hepatocytes resuspended with WE medium; **closed circle**, mouse received hepatocytes resuspended with WE medium plus EHS-gel). (B-D) Establishment of vascular network into the subcutaneous space. Microspheres incorporating different doses of aFGF were resuspended with an equal volume of WE medium and EHS-gel. Five micrograms MS were placed into the subcutaneous space of FVB/N mice and analyzed 10 days later. Histological analysis (hematoxylin-eosin staining) of subcutaneous space around the EHS-gel containing either aFGF-MS-G1 (B) or aFGF-MS-G3 (C). **Arrows** denote vessels including blood cells within the channel. (D) Number of vessels into the subcutaneous space around the aFGF microspheres. $^{\#}P < .001$ between aFGF-MS-G3 vs. other groups. (E) Mouse serum hAAT level after transplantation. Different groups of aFGF-MS were placed into the subcutaneous space, and hepatocytes were transplanted at the same location 10 days later. The relative level of hAAT was compared with the value obtained 3 days after the transplantation (**open triangle**, **closed triangle**, **closed circle**, **open square**; aFGF-MS-G1, aFGF-MS-G2, aFGF-MS-G3, aFGF-MS-G4, respectively). Note that aFGF-MS-G3, which induced high level of vascular network (see panel D), showed persistent survival of hepatocytes (**closed circle**).

mouse hepatocytes with or without co-transplanting EHS-gel. Although hepatocytes with the EHS-gel group showed significantly higher survival as compared with the non–EHS-gel group, the transplanted hepatocytes in both of these groups exhibited a sharp drop in survival over time (Fig. 4A). Based on the lack of sufficient vascular support for the transplanted hepatocytes (not shown), we hypothesized that establishing a local vascular network at the transplantation site would allow nutrient and gas transport to the grafts, and this would reduce graft loss.

To do this, we created polylactide-co-glycolide-co-polyethylene glycol MS incorporating different doses of a potent angiogenic agent, aFGF,[23] to provide continuous local delivery (aFGF-MS-G1 to G4). Five micrograms MS (resuspended in EHS-gel) were placed into the subcutaneous space of FVB/N mice, and histological analyses were performed by using subcutaneous tissue samples taken 10 days later. Quantitative increases in local tissue vascularity around the EHS-gel plug were demonstrated in the aFGF-MS-G3–treated animals, with the optimal dosage being a mean daily release of 0.167 ng (Fig. 4B-D). We then placed aFGF-MSs-G3 into the subcutaneous space and transplanted hepatocytes in EHS-gel in the same location 10 days later. When active vascular networks were induced with aFGF-MS-G3, persistent hepatocyte survival was achieved for the duration of this extended experiment (140 days) (Fig. 4E).

To further establish whether the engineered liver tissues in the subcutaneous space also possessed proliferative capacity, we applied the 2 different modes of proliferation (hepatectomy and DH) to mice 70 days after the hepatocyte engraftment by using another set of mice that also had been treated with aFGF-MS-G3. We delivered BrdU for 14 days from the day of the stimulus. Hepatocytes in

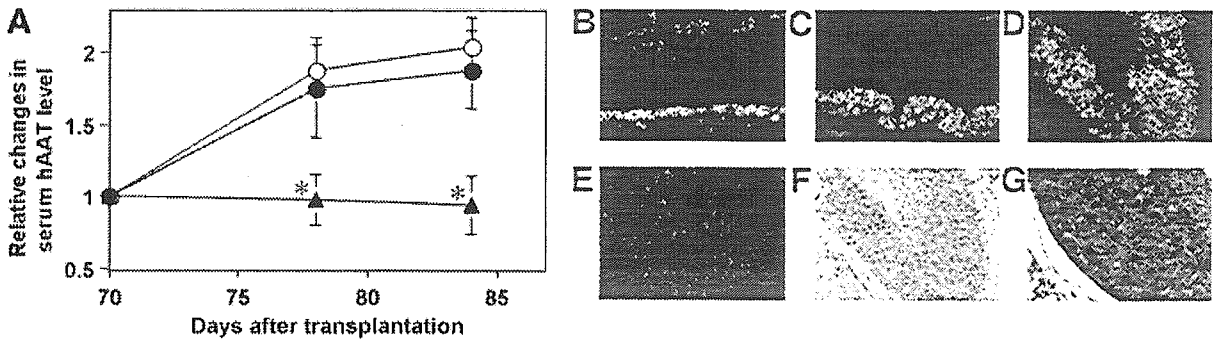

Fig. 5. Proliferation of the naïve liver and liver tissues into the subcutaneous space. Mice received aFGF-MS-G3 into the subcutaneous space and then received hepatocytes resuspended with WE medium plus EHS-gel 10 days later. At day 70, mice received either a two-third partial hepatectomy (hepatectomy group) (C), intragastric injection of TCPOBOP (DH group) (D), or nontreatment as a control (B). We delivered BrdU continuously for 14 days (days 70-84). (A) Mouse serum hAAT levels after the regeneration stimulus. At days 70, 78, and 84, the serum hAAT level was measured by enzyme-linked immunosorbent assay (ELISA), and the relative level of hAAT was expressed by comparing values with that of day 70 in each mouse. **Open circle**, mice in the hepatectomy group; **closed circle**, mice in the DH group; and **closed triangle**, mice in the control group. $*P < .05$ between WE medium plus EHS-gel group vs. WE medium group. (B-D) Representative photomicrographs of BrdU and hAAT co-immunostaining from engrafted hepatocytes in the subcutaneous sections of control group. hAAT-positive cytoplasm were colored with fluorescein isothiocyanate, and the BrdU-positive nuclei are colored with Texas red. (E) Representative photomicrographs of BrdU immunostaining from duodenum epithelium sections of control. BrdU-positive nuclei are colored with Texas red. All the epithelial cells that showed positive staining in their nuclei confirmed that BrdU had continuously been infused to the mice. (F-G) Histological analysis of the engineered liver tissues into the subcutaneous space in the DH group at day 84. HE staining (F) and PAS staining (G). Original magnification, ×100 (E); and ×200 (B-D and F-G).

the engineered liver tissues showed 10.5% ± 3.3%, 93.3% ± 4.7%, and 75.6% ± 6.7% BrdU labeling index in the control, hepatectomy, and DH groups, respectively (Fig. 5B-D; Table 1). Serum hAAT level at day 84 increased to 192% ± 21%, and 180% ± 19% in the hepatectomy and DH groups as compared with their value at day 70, whereas the control group did not show any increase (97.6% ± 5.2%) (Fig. 5A). Histological examination of the graft samples at day 84 confirmed that the hAAT was produced by the transplanted hepatocytes (not shown). After proliferation, the morphology and function of the transplanted cells as differentiated hepatocytes was again confirmed by hematoxylin & eosin (HE) and PAS staining for glycogen. (Fig. 5F-G).

Discussion

The present study shows that hepatocytes can be successfully engrafted and maintained for over 100 days at 2 distinct extrahepatic sites, under the kidney capsule and in the subcutaneous space. The persistency of the grafts at the subcutaneous space was only possible by establishing a vascular network before the transplantation induced by controlled local release of aFGF. We believe the combination of EHS gel and a vascular network provides a complex of matrix proteins and nutrients[24,25] that allows essential support for hepatocellular functions[26] and formation of hepatic organelles,[27] ultimately allowing for persistent generation of a functional extrahepatic organ *in vivo*.

Under-the-kidney capsule space has supported cell engraftment in the experiments of islet cell transplantation.[28] It was suggested that this site allowed rapid establishment of a vascular network that contributed to long-term cell survival. However, hepatocytes alone, grafted under the kidney capsule, have not shown persistent survival.[3,11] Such a difference might be explained by the difference in the nature of the cell types; especially once the hepatocytes are isolated from the liver, cells in culture will undergo a rapid process of de-differentiation leading to loss of function.[29] *In vitro* studies have suggested that providing extracellular matrix components, especially basement membrane proteins, including laminin and type IV collagen, is important for maintaining hepatocyte differentiated function.[26,29] In addition, others have found that EHS-gel has the ability to induce vascularization for a short period.[30] The EHS extracellular matrix gel is rich in basement membrane components, but it also contains a small amount of growth factors, such as epidermal growth factors. In our preliminary experiment, we compared the effect on the transplanted hepatocyte survival of the regular EHS-gel and growth factor reduced EHS-gel. We found there are no differences in these 2 EHS-gel components, suggesting that extracellular matrix components are the predominant contributory factors for the enhanced hepatocyte engraftment (data not shown). These studies clearly demonstrated that providing extracellular matrix components in the transplant setting is important for increasing the engraftment and

stable survival of the hepatocytes, leading to liver tissue engineering. However, further experiments are needed to analyze which of the extracellular matrix element(s) are necessary for facilitating hepatocyte engraftment.

Toward a novel treatment for liver diseases, we then assessed the therapeutic efficacy of our approach for liver tissue engineering in a mouse model of hemophilia A. Hemophilia A is a bleeding disorder, occurring in 1 of approximately 5,000 men who lack the production of functional factor VIII. Protein replacement therapy with infusion of plasma-derived or recombinant factor VIII has been a standard for this disease. Because the liver is a major contributory organ for factor VIII production,[31] recent experience in transplanting whole or part of the liver into hemophilia patients have resulted in curative levels (>50%) of factor VIII production and clotting activity.[32,33] However, raising these levels into the range of 2% to 3% will result in a significant phenotypic improvement in the disease, and this prompted us to establish whether engineering liver tissues would have a therapeutic benefit on hemophilia A.[34] As shown in this study, by engineering liver tissue with 3×10^6 hepatocytes that are equivalent to approx 3% of the naïve liver, we could demonstrate therapeutic efficacy in reconstituting 5% to 10% of normal clotting activity, enough to reduce the bleeding time to near normal values. These findings establish the proof-of-concept that extrahepatic liver tissue engineering is a viable therapy for patients with hepatodeficiency conditions.

The subcutaneous space is a particularly attractive site for cell transplantation and tissue engineering, because it is an easy site to access and manipulate, and it holds a remarkably large capacity for engrafting.[3,7] However, several studies have not been able to achieve persistent survival of hepatocytes transplanted into the subcutaneous space.[8,35] In the previous and present studies, we experienced a significant decrease in cell survival within the first 2 weeks after the transplantation even in the presence of an extracellular matrix component and HGF/cMet stimulation. We hypothesized that a major cause of cell death was insufficient vascularity at the transplantation site. Our strategy, establishing a vascular network using continuous delivery of aFGF before transplantation, clearly demonstrated its importance for persistent survival leading to liver tissue engineering. Other studies have reported that transplanting hepatocytes transfected with vascular endothelial growth factor genes or transplanting hepatocytes with a bFGF-releasing device showed some effects on survival when cells were transplanted into the abdominal cavity.[24,25] However, persistent survival of the hepatocytes was not achieved. In prior strategies, once cells were implanted in the recipient, metabolic needs began immediately, but it took several days for the growth of new blood vessels that would deliver oxygen and nutrients to the grafts.[7] Ready access to the subcutaneous space renders a staged procedure such as that presented here more clinically feasible.

The liver has a number of fascinating properties because of its proliferative capacity[18,36–38] through 2 distinct pathways, compensatory regeneration or direct hyperplasia.[19,20,39] A large number of molecules are involved in the liver proliferation process in both endocrine and paracrine fashions.[36,39] We have previously reported that the activation of HGF/cMet is one of the important pathways for hepatocytes to grow at the extrahepatic sites.[12] Although it has been suggested that shunting the portal circulation to the engrafted hepatocytes (to diverse growth factors from portal to a general circulation) is necessary for their cell proliferation,[40] the present study clearly demonstrates that engineered liver tissues at two different extrahepatic sites could regenerate with similar activity as their naïve livers without the need of portal blood supply. It is also important to note that the onset and completion of the proliferation process of the engineered liver tissues occurred within the same period as naïve liver. These findings, along with the morphological, and enzymatical (PAS staining) analyses, proved that the liver tissues comprising donor hepatocytes were recognized as a part of their own liver *in vivo*.

In summary, the present studies show that liver tissue, which was recognized as a part of the host naïve liver in terms of the proliferation profile, could be engineered at a heterologous site that does not have access to the portal circulation. This approach is further supported by the recent interest in the ability to generate mature hepatocytes from embryonic, hematopoietic, or somatic stem cells as an alternative cell source.[41] These cells could be transplanted in a similar manner, offering new medical therapy for many patients with a myriad of different diseases.[3,34] Taken together, the current work thus can serve as the basis to enable further development of tissue engineering, stem cell work, and molecular medicine approaches to liver disease.

Acknowledgment: The authors thank Dr. G.L. Bumgardner for providing the hA1AT-FVB/N mouse line, Dr. H. Kazazian Jr. for providing factor VIII–deficient mice, and Dr. B. Diwan for providing TCPOCOP. The authors also thank Thu Thao T. Pham, Kimbary Wiges, and Rika Hongo for technical assistance in histology and enzyme-linked immunosorbent assay.

References

1. Fox IJ, Chowdhury JR, Kaufman SS, Goertzen TC, Chowdhury NR, Warkentin PI, et al. Treatment of the Crigler-Najjar syndrome type I with hepatocyte transplantation. N Engl J Med 1998;338:1422–1426.

2. Muraca M, Gerunda G, Neri D, Vilei MT, Granato A, Feltracco P, et al. Hepatocyte transplantation as a treatment for glycogen storage disease type 1a. Lancet 2002;359:317–318.
3. Ohashi K, Park F, Kay MA. Hepatocyte transplantation: clinical and experimental application. J Mol Med 2001;79:617–630.
4. Ponder KP, Gupta S, Leland F, Darlington G, Finegold M, DeMayo J, et al. Mouse hepatocytes migrate to liver parenchyma and function indefinitely after intrasplenic transplantation. Proc Natl Acad Sci U S A 1991; 88:1217–1221.
5. Gupta S, Chowdhury JR. Hepatocyte transplantation. In: Arias IM, Boyer JL, Fausto N, Jakoby WB, Schachter D, Shafritz DA, eds. The Liver: Biology and Pathobiology. 3rd ed. New York, NY: Raven Press, 1994: 1519–1536.
6. Schneider A, Attaran M, Gratz KF, Bleck JS, Winkler M, Manns MP, et al. Intraportal infusion of 99mtechnetium-macro-aggregrated albumin particles and hepatocytes in rabbits: assessment of shunting and portal hemodynamic changes. Transplantation 2003;75:296–302.
7. Griffith LG, Naughton G. Tissue engineering-current challenges and expanding opportunities. Science 2002;295:1009–1014.
8. Ohashi K, Marion PL, Nakai H, Meusu L, Cullen JM, Bordier BB, et al. Sustained survival of human hepatocytes in mice: a model for in vivo infection with human hepatitis B and hepatitis delta viruses. Nat Med 2000;6:327–331.
9. Allen JW, Bhatia SN. Engineering liver therapies for the future. Tissue Eng 2002;8:725–737.
10. Jirtle RL, Michalopoulos G. Effects of partial hepatectomy on transplanted hepatocytes. Cancer Res 1982;42:3000–3004.
11. Ricordi C, Lacy PE, Callery MP, Park PW, Flye MW. Trophic factors from pancreatic islets in combined hepatocyte-islet allografts enhance hepatocellular survival. Surgery 1989;105(2 Pt 1):218–223.
12. Ohashi K, Meuse L, Schwall R, Kay MA. cMet activation allows persistent engraftment of ectopically transplanted xenogenic human hepatocytes in mice. Transplant Proc 2001;33:587–588.
13. Bi L, Lawler AM, Antonarakis SE, High KA, Gearhart JD, Kazazian HH Jr. Targeted disruption of the mouse factor VIII gene produces a model of haemophilia A. Nat Genet 1995;10:119–121.
14. Shima M, Matsumoto T, Fukuda K, Kubota Y, Tanaka I, Nishiya K, et al. The utility of activated partial thromboplastin time (apt) clot waveform in the investigation of hemophilia A patients with very low levels of factor VIII activity (FVIII:C). Thromb Haemost 2002;87:436–441.
15. Wang L, Zoppe M, Hackeng TM, Griffin JH, Lee KF, Verma IM. A factor IX-deficient mouse model for hemophilia B gene therapy. Proc Natl Acad Sci U S A 1997;94:11563–11566.
16. Yuksel E, Weinfeld AB, Cleek R, Waugh JM, Jensen J, Boutros S, et al. De novo adipose tissue generation through long-term, local delivery of insulin and insulin-like growth factor-1 by PLGA/PEG microspheres in an in vivo rat model: a novel concept and capability. Plast Reconstr Surg 2000;105: 1721–1729.
17. Elkins C, Waugh JM, Amabile PG, Minamiguchi H, Uy M, Sugimoto K, et al. Development of a platform to evaluate and limit in-stent restenosis. Tissue Engineering 2002;8:395–407.
18. Ponder KP, Gupta S, Leland F, Darlington G, Finegold M, Demayo J, et al. Mouse hepatocytes migrate to liver parenchyma and function indefinitely after intrasplenic transplantation. Proc Natl Acad Sci U S A 1991; 88:1217–1221.
19. Ohashi K, Park F, Kay MA. Role of hepatocyte direct hyperplasia in lentivirus-mediated liver transduction in vivo. Hum Gene Ther 2002;13: 653–663.
20. Columbano A, Ledda-Columbano GM, Pibiri M, Piga R, Shinozuka H, DeLuca V, et al. Increased expression of c-fos, c-jun and LRF-1 is not required for in vivo priming of hepatocytes by the mitogen TCPOBOP. Oncogene 1997;14:857–863.
21. Ohashi K, Tsutsumi M, Tsujiuchi T, Kobitsu K, Okajima E, Nakajima Y, et al. Enhancement of N-nitrosodiethylamine-initiated hepatocarcinogenesis caused by a colchicines-induced cell cycle disturbance in partially hepatectomized rats. Cancer Res 1996;56:3474–3479.
22. Bumgardner GL, Heininger M, Li J, Xia D, Parker-Thornburg J, Ferguson RM, et al. A functional model of hepatocyte transplantation for in vivo immunologic studies. Transplantation 1998;65:53–61.
23. Passaniti A, Taylor RM, Pili R, Guo Y, Long PV, Haney JA, et al. A simple, quantitative method for assessing angiogenesis and antiangiogenic agents using reconstituted basement membrane, heparin, and fibroblast growth factor. Lab Invest 1992;67:519–528.
24. Ajioka T, Akaike T, Watanabe Y. Expression of vascular endothelial growth factor promotes colonization, vascularization, and growth of transplanted hepatic tissues in the mouse. HEPATOLOGY 1999;29:396–402.
25. Lee H, Cusick RA, Browne F, Ho Kim T, Ma PX, Utsunomiya H, et al. Local delivery of basic fibroblast growth factor increases both angiogenesis and engraftment of hepatocytes in tissue-engineered polymer devices. Transplantation 2002;73:1589–1593.
26. Bissell DM, Arenson DM, Maher JJ, Roll FJ . Support of cultured hepatocytes by a laminin-rich gel: evidence for a functionally significant subendothelial matrix in normal rat liver. J Clin Invest 1987;79:801–812.
27. Mitaka T, Sato F, Mizuguchi T, Yokono T, Mochizuki Y. Reconstruction of hepatic organoid by rat small hepatocytes and hepatic nonparenchymal cells. HEPATOLOGY 1999;29:111–125.
28. Kumagai N, O'Neil JJ, Barth RN, LaMattina JC, Utsugi R, Moran SG, et al. Vascularized islet-cell transplantation in miniature swine. I. Preparation of vascularized islet kidneys. Transplantation 2002;74:1223–1230.
29. Runge D, Runge DM, Drenning SD, Bowen WC Jr, Grandis JR, Michalopoulos GK. Growth and differentiation of rat hepatocytes: changes in transcription factors HNF-3, HNF-4, STAT-3, and STAT-5. Biochem Biophys Res Commun 1998;250:762–768.
30. Fridman R, Sweeney TM, Zain M, Martin GR, Kleinman HK. Malignant transformation of NIH-3T3 cells after subcutaneous co-injection with a reconstituted basement membrane (Matrigel). Int J Cancer 1992;51:740–744.
31. Wion KL, Kelly D, Summerfield JA, Tuddenham EG, Lawn RM. Distribution of factor VIII mRNA and antigen in human liver and other tissues. Nature 1985;317:726–729.
32. Wilde J, Teixeira P, Bramhall SR, Gunson B, Mutimer D, Mirza DF. Liver transplantation in haemophilia. Br J Haematol 2002;117:952–956.
33. Horita K, Matsunami H, Shimizu Y, Shimizu A, Kurimoto M, Suzuki K, et al. Treatment of a patient with hemophilia A and hepatitis C virus-related cirrhosis by living-related liver transplantation from an obligate carrier donor. Transplantation 2002;73:1909–1912.
34. High KA. Gene therapy: a 2001 perspective. Hemophilia 2001;7(Suppl 1):23–27.
35. Demetriou AA, Whiting JF, Feldman D, Levenson SM, Chowdhury NR, Moscioni AD, et al. Replacement of liver function in rats by transplantation of microcarrier-attached hepatocytes. Science 986;233:1190–1192.
36. Michalopoulos GK, DeFrancis ME. Liver regeneration. Science 1997;276: 60–66.
37. Ohashi K, Tsutsumi M, Nakajima Y, Kobitsu K, Nakano H, Konishi Y. Telomere changes in human hepatocellular carcinomas and hepatitis virus infected noncancerous livers. Cancer 1996;77: S1747–S1751.
38. Higgins GM, Anderson RM. Experimental pathology of the liver: restoration of the liver of the white rat following partial surgical removal. Arch Pathol 1931;12:186–202.
39. Columbano A, Shinozuka H. Liver regeneration versus direct hyperplasia. FASEB J 1996;10:1118–1128.
40. Kaufmann PM, Sano K, Uyama S, Takeda T, Vacanti JP. Heterotopic hepatocyte transplantation: assessing the impact of hepatotrophic stimulation. Transplant Proc 1994;26:2240–2241.
41. Jones EA, Tosh D, Wilson DI, Lindsay S, Forrester LM. Hepatic differentiation of murine embryonic stem cells. Exp Cell Res 2002;272:15–22.

Disorders of Hemostasis • Research Paper

Association of anti-idiotypic antibodies with immune tolerance induction for the treatment of hemophilia A with inhibitors

[haematologica]
2004;89:696-703

YOSHIHIKO SAKURAI
MIDORI SHIMA
ICHIRO TANAKA
KAZUYOSHI FUKUDA
KOICHI YOSHIDA
AKIRA YOSHIOKA

ABSTRACT

Background and Objectives. Hemophilia A patients with inhibitors can be treated effectively with immune tolerance induction therapy (ITI). One of the underlying mechanisms of ITI is conceived to be a neutralizing activity of anti-idiotypic antibodies on inhibitors. The goal of the present study was to develop an uncomplicated method for assessing anti-idiotypic antibodies and to prove the advent of anti-idiotypic antibodies in ITI.

Design and Methods. We studied a total of 26 plasma samples obtained from 9 hemophilic inhibitor patients who were treated with ITI. The samples were investigated with a novel method for detecting anti-idiotypic antibodies based on a liquid phase blocking immunoprecipitation.

Results. Plasma anti-factor VIII (FVIII) antibody titer was reduced by adding plasma from patients who had received completely successful ITI. This anti-FVIII antibody-neutralization activity of the plasma was impaired by treating the plasma with protein G beads. In addition, treating inhibitor plasma from patients in whom ITI had been unsuccessful with FVIII affinity beads resulted in the development of the anti-FVIII antibody-neutralization activity. Furthermore, the anti-FVIII antibody-neutralization activity of anti-FVIII antibody-depleted plasma obtained in a late period of ITI on inhibitor plasmas obtained during ITI increased over time.

Interpretation and Conclusions. Our results suggest that; (i) plasma from patients in whom ITI was completely successful contained an anti-FVIII antibody-neutralization factor; (ii) the anti-FVIII antibody-neutralization factor was in the IgG fraction (i.e., the factor would be anti-idiotypic antibodies), and (iii) anti-idiotypic antibodies existed even in plasma from patients in whom ITI was unsuccessful. Our observations support the notion that the mechanism of ITI is associated with the development of anti-idiotypic antibodies.

Key words: hemophilia A, antiidiotypic antibody, immune tolerance induction therapy, affinity maturation.

From the Department of Pediatrics, Nara Medical University, Nara, Japan.

Correspondence: Yoshihiko Sakurai, M.D., Ph.D. Department of Pediatrics, Nara Medical University, 840 Shijo-cho, Kashihara, Nara 634-8522, Japan. E-mail: ysakurai@naramed-u.ac.jp

The development of factor VIII (FVIII) inhibitors remains a serious clinical complication arising from the treatment of hemophilia A patients. A recent meta-analysis revealed that the average cumulative incidence of FVIII inhibitors is 15-52%.[1-5] Once an inhibitor develops, treatment for bleeding episodes is difficult, particularly in high responder patients. The main goal of the treatment of patients with hemophilia A who have inhibitors is to eradicate the inhibitor. For this purpose, induction of immune tolerance (ITI) to FVIII therapy is the most promising strategy. In 1977, Brackmann and Gormsen reported a curative ITI protocol for inhibitor patients.[6] The protocol, known as the Bonn Protocol, is based on administration of high doses of FVIII (150 IU/kg twice a day). In 1999, Oldenburg *et al.* reported the outcome of 60 hemophilia A inhibitor patients treated according to the Bonn Protocol. Successful immune tolerance was achieved in 52 patients (86.7%), while the therapy failed in eight patients (13.3%).[7] Furthermore, several studies have been performed using a modified dosage scheme[8-9] and the outcome of the low-dose ITI protocol was reported to achieve a similar success rate to that of the Bonn Protocol.[10] However, the mechanism by which immune tolerance is induced towards the inhibitor antibodies in hemophilia patients with inhibitors is controversial. Broadly speaking, tolerance has been hypothesized to be induced by several mechanisms:[11,12] clonal deletion,[13] clonal anergy, clonal ignorance, receptor editing,[14] suppressor cells, and anti-idiotype antibody.[15,16] Clonal deletion is the removal of immune response cells through programmed cell death or apoptosis. In clonal anergy, immune response cells are alive but

fail to respond to antigen challenge. In these conditions, a cellular immune response can no longer exist. Clonal ignorance is a state in which immune response cells are alive and able to respond to antigen challenge, but do not see antigen because it is observed in immunologically privileged sites including the central nervous system, eye, and testis. In receptor editing, as an immature B cell grows and divides, its antibodies slowly mutate and change structure so that they no longer bind the antigen and would not be eliminated or inactivated. Furthermore, the antigen may induce suppressor T cells that can suppress immune responses of both B and T cells. Although all the possible mechanisms could result in successful ITI, some investigators suggest that anergy induced by cross-linking surface immunoglobulins such as anti-idiotypic antibodies can achieve immune tolerance.[12]

The presence of anti-idiotypic antibodies reacting with FVIII:C inhibitors in intravenous immunoglobulin preparations has been reported since 1984.[17-20] These preparations are used as a treatment for spontaneous FVIII:C inhibitors, i.e. acquired hemophilia.[21] Furthermore, it has been suggested that anti-idiotypic antibodies play a role in the down-regulation of anti-FVIII antibody production as well as inhibiting the binding of antibodies to FVIII in the ITI.[22] The method used in the previous studies to detect the anti-idiotypic antibodies did reveal their presence, but has the drawbacks that it needs complicated and time-consuming column operations and is based on a solid phase immunoassay. The fluctuation of production of anti-idiotypic antibodies during the course of ITI therapy remains unclear. The aim of the present study was to establish a simple method for assessing anti-idiotypic antibodies and to elucidate the role of such antibodies in ITI. We present the possibility that an idiotypic network is associated with ITI.

Design and Methods

Patients

In this study, we investigated a total of 26 plasma samples obtained from 9 hemophilic inhibitor patients who were treated with ITI using highly purified FVIII concentrate derived from human plasma. This work was approved by the institutional review board of Nara Medical University. All plasma samples were obtained from the patients who had given informed consent.

Bethesda and immunoprecipitation assays

Plasma samples were analyzed by the Bethesda assay[23] for inhibitory antibodies and/or through the more sensitive immunoprecipitation (IP) assay for all anti-FVIII antibodies. The latter assays were performed as previously described.[24] In brief, 7 μg of FVIII in 20 μL of 0.2 M sodium acetate buffer (pH 6.8) were ^{125}I-labeled with IODO-Gen Pre-Coated Iodination Tube (Pierce Biotechnology, Rockford, IL, USA), according to the manufacturer's instructions. Specific radioactivities ranged from 3.4 to 4.5 μCi/μg. Duplicates of 50 μL inhibitor plasma dilutions in 20 mM Tris, 0.15 M NaCl, pH 7.4 (TBS), and 1% bovine serum albumin (BSA) were incubated with 10 μL ^{125}I-labeled FVIII (0.75 nM, final concentration) at 4°C overnight with agitation, and for 2 more hours after addition of 100 μL TBS dilution buffer and 50 μL of a suspension of protein G-Sepharose beads (Amersham Biosciences, Piscataway, NJ, USA). After washing the beads three times with TBS-0.05% Tween 20, bound radioactivity was determined in a gamma counter (ARC-380, Aloka, Tokyo, Japan). Background radioactivity without antibody was 1% to 2%, and maximal binding with antibody was 60% to 70%. Results were expressed as immunoprecipitation units per milliliter (IPU/mL), being calculated as: 1 - (bound/total radioactivity - background) × plasma dilution × 16.7 (to convert to IPU/mL).

Detection of anti-FVIII antibody-neutralization activities in patients' plasma

The assays used in this study are based on a novel liquid phase blocking IP method, and specific neutralization of a defined IP titer of anti-FVIII antibody was detected using anti-FVIII antibody-neutralization factors (i.e., presumably anti-idiotypic antibodies) in the test sample. After the test plasma had been allowed to react with inhibitor plasma (i.e., positive BU titer plasma), the mixture of the test plasma and inhibitor plasma was transferred to a tube containing protein G-Sepharose beads for the IP assay. The presence of anti-FVIII antibody-neutralization factors in the test plasma would result in the formation of immune complexes, such as complexes of probable anti-FVIII antibodies-anti-idiotypic antibodies, and consequently reduce the amount of free anti-FVIII antibodies trapped by the protein G-Sepharose beads. After washing the beads and adding radiolabeled FVIII, radioactivity (i.e., IP titer) was measured: a reduction was observed when anti-FVIII antibody-neutralization factors were present.

Firstly, in order to detect anti-FVIII antibody-neutralization factors in a patient's plasma, plasma from a patient who had undergone successful ITI was mixed with an equal volume of plasma from the same patient showing positive inhibitors prior to ITI (Figure 1A). The mixture was incubated at 4°C with agitation overnight, and anti-FVIII antibody titer of the mixture was measured by the IP assay. In all mixing studies, inhibitor plasma samples that showed a value of more than 10

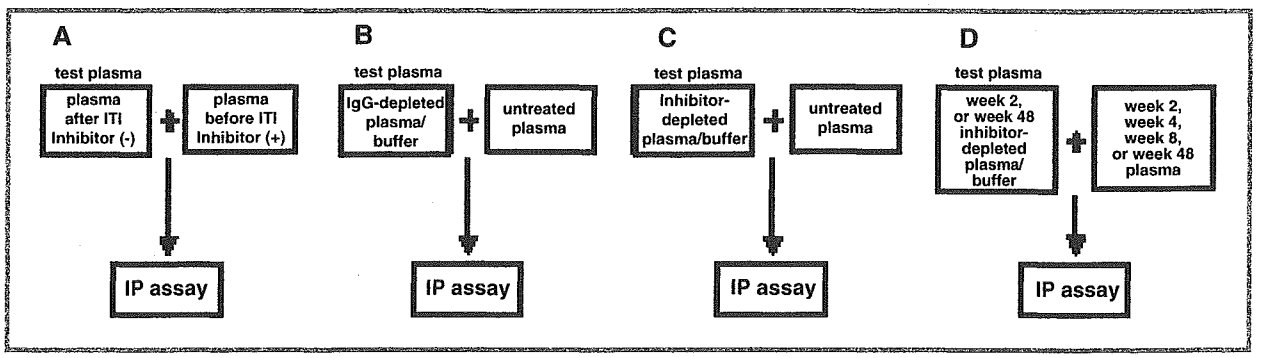

Figure 1 Detection of anti-FVIII antibody-neutralization activities.

IPU/mL were adjusted to give values of less than 10 IPU/mL.

Secondly, to confirm that the anti-FVIII antibody-neutralization factors in the patient's plasma were in immunoglobulins (IgGs), sample plasma pretreated with protein G-Sepharose beads (IgG-depleted plasma) or buffer A as control (30 mM $CaCl_2$, in 10 mM Tris-HCl, pH 7.2) was mixed with an equal volume of the same plasma without the protein G-Sepharose bead treatment (Figure 1B). The protein G-Sepharose beads for the elimination of IgGs were washed three times with one volume of buffer A containing 0.1% BSA, followed by 3 washes with one volume of buffer A without BSA. Fifty microliters of the patient's plasma were mixed with an equal volume of protein G-Sepharose beads (50% slurry) and incubated at 4°C with agitation overnight. Samples were centrifuged at 250×g for 3 min, and the supernatant was recovered as IgG-depleted sample plasma. The mixture of 50 μL of the patient's plasma and 25 μL of buffer A was incubated at 4°C with agitation overnight. This solution was used as a reference. The solutions were mixed with an equal volume of plasma from the same patient and incubated at 4°C with agitation for 3 hours. Anti-FVIII antibody titer was then measured by the IP assay.

Thirdly, to elucidate whether anti-FVIII antibody-neutralization antibodies existed in the patient's plasma, sample plasma pretreated with FVIII-Sepharose (i.e., anti-FVIII antibody-depleted plasma) or buffer A (control) was mixed with an equal volume of the same plasma without the FVIII-Sepharose treatment (Figure 1C). Sample plasmas were collected before ITI (patient D) and during ITI from the patients who received incompletely successful ITI (patients E, F, and G), and unsuccessful ITI (patients H and I). FVIII-Sepharose for elimination of anti-FVIII antibody was prepared. FVIII (3 mg) was coupled to 1 g CNBr-activated Sepharose 4B (Amersham Biosciences) in coupling buffer (0.1 M $NaHCO_3$ containing 0.5 M NaCl, pH 8.3) at 4°C for 18 hours. Prior to use, the FVIII-Sepharose beads were washed three times with one volume of buffer A containing 0.1% BSA, followed by 3 washes with one volume of buffer A without BSA. Fifty μL of the patient's plasma were mixed with an equal volume of FVIII-Sepharose (50% slurry) and incubated at 4°C overnight with agitation. Samples were centrifuged at 250×g for 3 min, and the supernatant was recovered as anti-FVIII antibody-depleted sample plasma. The mixture of 50 μL of patient's plasma and 25 μL of buffer A was also incubated at 4°C with agitation overnight. This solution was used as a reference. The solutions were mixed with equal volume of the same patient's plasma and incubated at 4°C with agitation for 3 hours. Anti-FVIII antibody titer was measured by the IP assay.

Table 1 Inhibitor titer and outcomes of ITI in 9 inhibitor patients with hemophilia A.

	Weeks	*BU/mL*	*IPU/mL*	*Outcomes*
A	Before	2	52.5	
	After	0	0	
B	Before	1	85.6	Completely successful
	2	6	504	
	After	0	0	
C	Before	0	3.8	
	28	2	40.5	
	After	0	0	
D	Before	0	45.6	
	After	0	6.4	
E	Before	12	1644	
	3	234	12560	
	After	0	5.6	
F	2	44	3008	Incompletely successful
	4	23	684	
	8	2	148	
	After	0	3.6	
G	1	284	7890	
	2	756	19800	
	After	0	4.6	
H	1	1	7.6	
	2	123	940	
	After	30,4	528	Unsuccessful
I	1	930	30230	
	13	78	7340	
	After	2	48.8	

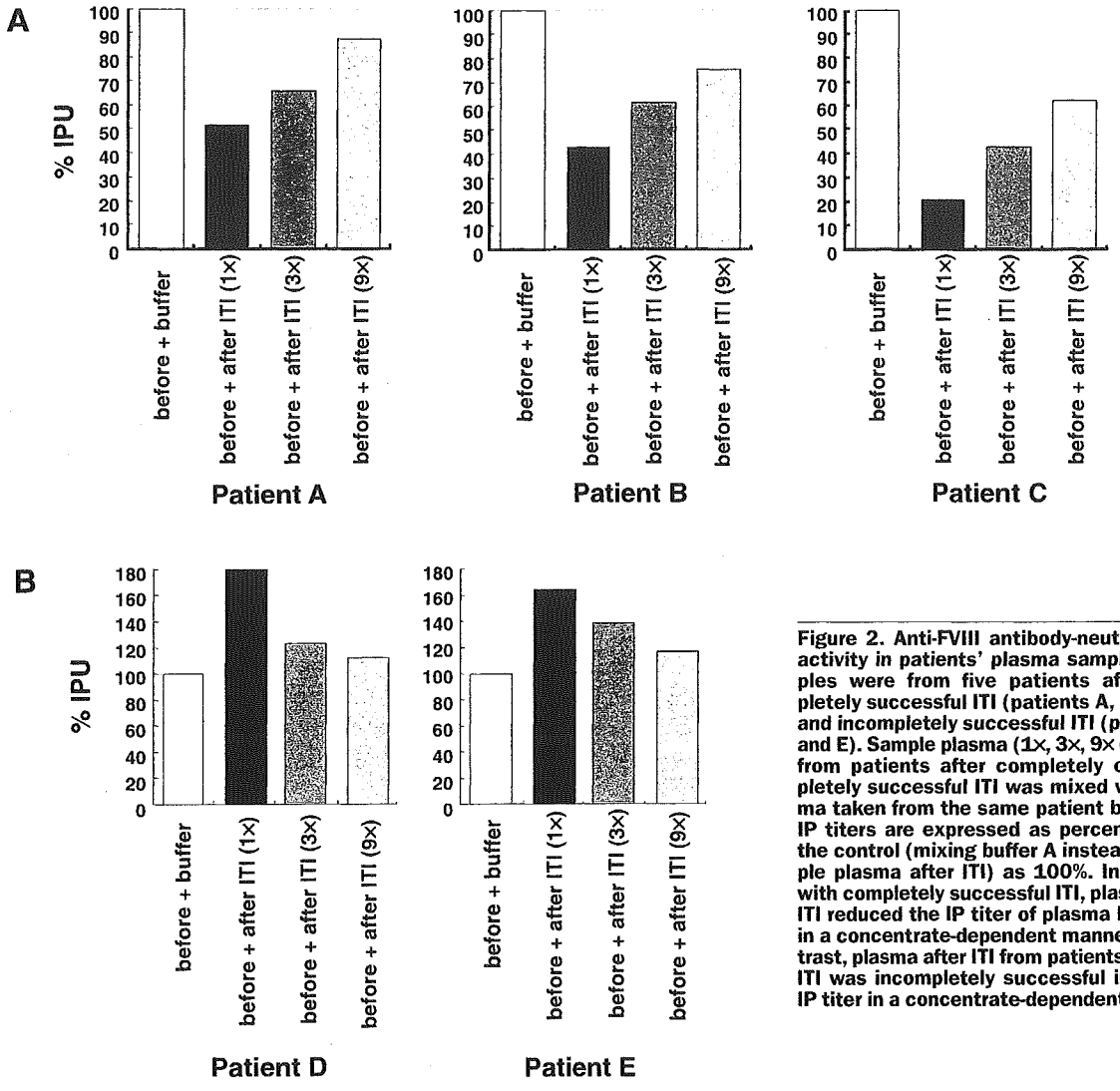

Figure 2. Anti-FVIII antibody-neutralization activity in patients' plasma samples. Samples were from five patients after completely successful ITI (patients A, B, and C) and incompletely successful ITI (patients D and E). Sample plasma (1×, 3×, 9× dilutions) from patients after completely or incompletely successful ITI was mixed with plasma taken from the same patient before ITI. IP titers are expressed as percent, taking the control (mixing buffer A instead of sample plasma after ITI) as 100%. In patients with completely successful ITI, plasma after ITI reduced the IP titer of plasma before ITI in a concentrate-dependent manner. In contrast, plasma after ITI from patients in whom ITI was incompletely successful increased IP titer in a concentrate-dependent manner.

Lastly, anti-FVIII antibody-depleted plasma obtained 2 and 48 weeks after the start of ITI or buffer A (control) was mixed with plasma obtained at four sampling points (week 2, 4, 8 and 48) during ITI from a patient who underwent incompletely successful ITI (Patient F) (Figure1D). Week 48 corresponds to the completion of ITI in this patient. After the mixture had been incubated at 4°C with agitation overnight, anti-FVIII antibody titer was measured by the IP assay.

Results

Inhibitory antibody and anti-FVIII antibody titer of patients

We investigated a total of 26 plasma samples from 9 hemophilic inhibitor patients who were treated with ITI (Table 1). Depending on BU and IP titers, patients were categorized into 3 groups, those in whom ITI was *completely successful*, whose IP and BU titers were undetectable in plasma after ITI, those in whom ITI was *incompletely successful* whose BU titer was undetectable but IP titer was still detected after ITI, and those in whom ITI was *unsuccessful* whose BU titer was detectable after ITI. The ITI was completely successful in three patients (A, B, and C), incompletely successful in four (D, E, F, and G) and unsuccessful in two (H and I).

Presence of anti-FVIII antibody-neutralization factor in the plasma from patients with completely successful ITI

Addition of plasma after ITI from patients with completely successful ITI to plasma taken from the same patients during ITI reduced IP titer in a dose-dependent manner (Figure 2A). On the other hand, the addition of plasma after ITI from two patients with incompletely successful ITI to plasma taken from the same patients during ITI produced a higher IP titer than that

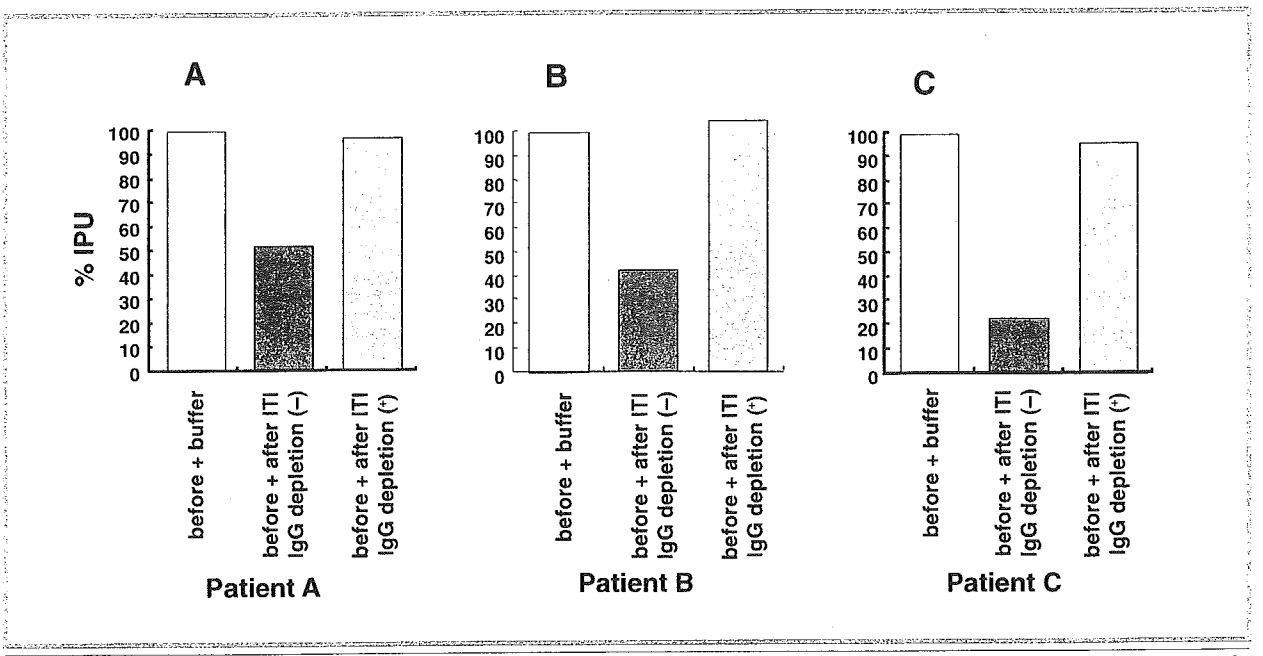

Figure 3. Effects of IgG depletion on inhibitor-neutralization activity. Samples were from three patients after completely successful ITI. IgGs were depleted from sample plasma using protein G-Sepharose beads. Sample plasma after ITI with/without IgG depletion was mixed with plasma taken from the same patient before ITI. IP titers are expressed as percent, taking the control (mixing buffer A instead of sample plasma after ITI) as 100%. In all cases, although sample plasma without IgG depletion after completely successful ITI did not affect IP titer, IgG depletion of sample plasma resulted in a reduction of the IP titer.

following addition of buffer A (control) (Figure 2B). This indicates that plasma from patients in whom ITI was completely successful contained some anti-FVIII antibody-neutralization factors.

Identification of anti-FVIII antibody-neutralization factor as IgGs

The effects of IgG-depleted plasma on IP titer of untreated plasma were investigated using plasma samples from the 3 patients in whom ITI had been completely successful. While plasma without protein G-Sepharose treatment reduced binding of antibodies to FVIII, IgG-depleted plasma did not influence it (Figure 3). Elimination of IgGs resulted in the loss of anti-FVIII antibody-neutralization effects, indicating that anti-FVIII antibody-neutralization factor would fall within IgGs. This implies that the plasma from patients with completely successful ITI contained IgGs against anti-FVIII antibodies, i.e. anti-idiotypic antibodies.

Anti-idiotypic antibodies existing in plasma during ITI

We also assessed the effects of anti-FVIII antibody-depleted plasma on IP titer of untreated plasma. All anti-FVIII antibody-depleted plasma samples reduced binding of antibodies to FVIII, while plasma without FVIII-Sepharose treatment did not influence, or even increased binding of antibodies to FVIII (Figure 4). These

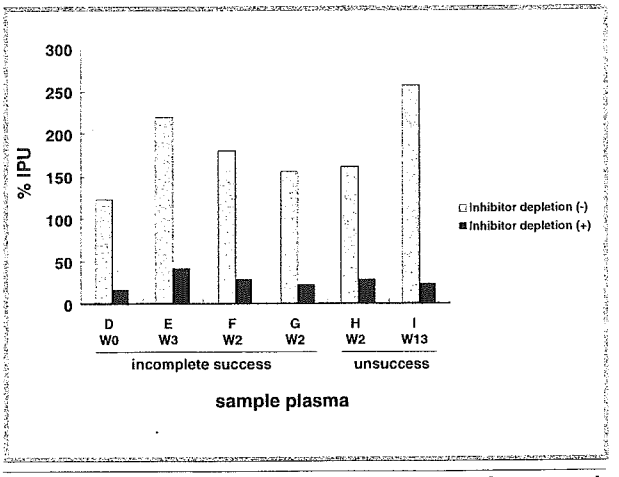

Figure 4. Effects of anti-FVIII antibody depletion on anti-FVIII antibody-neutralization activity. Samples were from four patients before (patient D, week 0) and during (patients E, week 3; patient F, week 2; and patient G, week 2) incompletely successful ITI, and from two during unsuccessful ITI (patients H, week 2; and patient I, week 13). Anti-FVIII antibodies were depleted from sample plasma using FVIII-Sepharose beads. Sample plasma before/during ITI with/without anti-FVIII antibody depletion was mixed with plasma obtained at the corresponding time point. IP titers are expressed as a percent, taking the control (mixing buffer A instead of sample plasma) as 100%. In all cases, although sample plasma without FVIII-Sepharose treatment increased IP titer, anti-FVIII antibody depletion from sample plasma resulted in a reduction of the IP titer.